Effects of Nuclear-Targeted Nanoparticles on the Cell Function in Human Oral Squamous Cell Carcinoma Cells During Cisplatin Treatment

A Thesis
Presented to
The Academic Faculty

By

Breanna Mann

In Partial Fulfillment
of the Requirements for the Research Option
School of Chemistry and Biochemistry

Georgia Institute of Technology
April 2020

Effects of Nuclear-Targeted Nanoparticles on the Cell Function in Human Oral Squamous Cell Carcinoma Cells During Cisplatin Treatment

Approved by:

Dr. Mostafa El-Sayed
School of Chemistry and Biochemistry
Georgia Institute of Technology

Dr. Alfred Merrill
School of Biology
Georgia Institute of Technology

Dr. Angus Wilkinson
School of Chemistry and Biochemistry
Georgia Institute of Technology

April 28, 2020

Acknowledgements

I would like to thank my research mentors, Dr. Nasrin Hooshmand and Dr. Sajanal Panikkanvalappil along with the head of the Laser Dynamics Laboratory, Dr. Mostafa El-Sayed for their mentorship and guidance throughout my undergraduate career. I would also like to thank my parents for their continued support throughout my career.

Table of Contents

Abstract

This project focuses on evaluating the effects of nanoparticles on the cellular responses in human oral squamous cell carcinoma (HSC) cells during the administration of cisplatin. Cisplatin is an effective chemotherapeutic drug used to treat numerous forms of human cancer. It is, however, also highly susceptible to creating drug resistance in cancer cells. Restriction of the mobility of HSC cells reduces its ability to spread resistant cells throughout the body. In this study, we investigated the cellular mobility of HSC cells in the presence of a combination of cisplatin and nuclear-targeted gold nanocubes. The HSC cells were treated with cisplatin with and without nanocubes to study their effects on the mobility. Trends were assessed for changes in position and velocity over time. It was found that, the presence of nanoparticles alone restricts the displacement of the HSC cells. As an extension, the effects of nanoparticles on drug resistant HCS cells was studied. HSC cells were systematically treated with cisplatin to create cisplatin-resistant cell lines. The viability of these cell lines were then tested at different levels of drug resistance. Furthermore, the effect of nuclear-targeted nanoparticles on bypassing drug resistance in cisplatin-resistant HSC cells were evaluated. Trends amongst cell resistance and nanoparticle presence were assessed. Furthermore, the radius and surface charge were analyzed to understand characteristics that lead to optimal uptake. Additionally, the growth and changes in uptake experienced by cisplatin resistant cells were analyzed to gain insight into how these changes effected uptake of the nanoparticles.

Introduction

Gold nanoparticles provide an innovative method of drug delivery that can be created in many different shapes, sizes, and materials. Different physical characteristics of the nanoparticles lead to different applications. One such application is the use of nanoparticles in a variety aspects of biological systems--particularly as a nanomedicine-- with functions ranging from sensors to imaging to delivery vehicles[1]. An area where these methods are being tested is cancer treatment. These nanoparticles have been used to deliver chemotherapeutics or act as a treatment themselves when combined with thermal radiation[2]. The use of nanoparticles as a means of drug delivery has been studied in many ways[1]. This study investigates the application of gold nanoparticles in combination with cisplatin, a common chemotherapeutic, and their combined therapeutic application within human oral squamous cell carcinoma cells. The use of gold as a material for this study is due to its enhanced biological properties which can be combined with photothermic abilities[3]. The optimization of nanoparticles for increased uptake, specifically within human oral squamous cell carcinoma cells, is explored throughout this study. The trade-off between the binding of different ligands (molecules which are bound to the exterior of the nanoparticle) and the surface charge are assessed within this study to determine the optimal surface for increased nanoparticle uptake. While the binding of the ligands can reduce cytotoxicity and allows for localization, it also changes the nanoparticle's surface charge. Different surface charges can lead to improper uptake if the charge is too negative. Moreover, the uptake of nanoparticles into cisplatin-resistant human oral squamous cell carcinoma cells is analyzed. The addition of the nanoparticles can allow for an increase in intracellular drug concentration due to a more effective uptake and faster drug release which can offset the effects of the resistivity. As photothermal therapy has previously been shown to be an effective treatment, this effectiveness is further

expanded upon for its application for cisplatin-resistant human oral squamous cell carcinoma cells. This study aims to increase the cellular uptake of gold nanoparticles in cisplatin resistant cells which in turn has the potential to overcome cisplatin resistance.

Throughout this study, the nanoparticles were assessed in human oral squamous cell carcinoma cells and in cisplatin resistant cells. Cisplatin is an anticancer drug that is effective due to its ability to enter the cell through multiple pathways by activating or silencing several genes. Once inside the cell, cisplatin effects DNA repair mechanisms leading to DNA damage and eventually apoptosis[4]. Cisplatin however has little selectivity for tumor versus normal tissue which limits the amount that can be used without detrimental side effects[5]. Dose limiting, in an effort to counteract the effects on normal tissue, leads to nephrotoxicity, myelosuppression, and chronic neurotoxicity and eventually an acquired resistance[6]. In many cases, cisplatin is combined with other therapies in attempts to overcome drug resistance and reduce toxicity[7]. Due to the complexity in which cisplatin interacts with the cell, the cisplatin resistance also arises from several separate and complex alternations[8]. With so many varied factors combining to lead to resistance, it can be hard to combat this resistance and find effective ways to treat resistant cells which is the main source of failure in cisplatin treatment[9]. One of the changes that appears in the resistant cells is differences in the cell surface and changes in cell surface binding sites[10]. The main method of cellular accumulation of cisplatin is using transporters on the cell's surface however resistant cells with different transporters cannot uptake the cisplatin. In this study, cisplatin was neither bound to the nanoparticle nor contained within the nanoparticle. Instead, they were both administered at the same time. The addition of the nanoparticles can allow for an increase in intracellular drug concentration due to a more effective uptake and faster drug release which can offset the effects of the resistivity. Nanoparticles are not moved across the cell membrane in the same way that

cisplatin is; in fact, nanoparticles can uptake into the cell through several different pathways of their own[11]. This study aims to discover a way to increase the cellular uptake of nanoparticles in cisplatin resistant cells which in turn has the potential to overcome cisplatin resistance.

Nanoparticles can be composed of different metal combinations such as gold, silver, and a gold-silver alloy, yet gold nanoparticles have been the most thoroughly studied and have many more applications in biological systems[3, 12]. Gold nanoparticles have been shown to convert light into heat which allows them to be used in photothermal therapeutics in which a laser is used to excite the nanoparticle and in turn induce apoptosis, cell death, of the targeted cell. Many studies are focusing solely on the use of gold nanoparticles due to these properties and have seen success. Accomplished gold nanoparticle photothermal therapy has been shown in pilot therapies to completely eradicate cancer in over 50% of the mice treated and show no sign of reoccurrence even two weeks later[13]. Another study has moved to clinical trials following success using photothermal therapy on gold nanoshells to fully remove surface tumors[14]. A photothermal approach that induces hyperthermia in glioblastoma, an aggressive brain cancer, has even been clinically approved in Europe[14]. Throughout this study, gold nanoparticles were used due to their enhanced biological properties which decrease their inherent toxicity to cells combined with photothermic abilities. Nanoparticles on their own cannot, however, freely enter the cell but must instead be conjugated with different ligands to make the nanoparticles cell viable. By changing the ratios of these different ligands on the surface of the nanoparticles, their uptake can be optimized. The first part of this study was designed to find the optimal ratio to have optimal uptake for each given cell type. Though this process has been shown before, particularly for cancers that are not deep tissue, it has not been done thoroughly for human oral squamous cell carcinoma cells. One of the best ways to assist with the uptake of the nanoparticle is by conjugating it with different

ligands that increase its cell viability, reducing barriers to entry, and causing localization within the cell following uptake. This study determines the optimal ratio for uptake into human oral squamous cell carcinoma cells by conjugating nanoparticles in various ratios of ligands and assessing the differences in uptake through dark-field imaging.

One of the ligands which can increase cell viability is polyethylene glycol, or PEG. In this study, the PEG ligand provides many different functions[15]. One function is to create steric repulsion so that when the nanoparticle is in proximity to other nanoparticles, there is less risk of aggregation[16]. Other functions are to minimize the cytotoxicity of the nanoparticles and to stabilize the nanoparticles. In past experimentation, PEG has been shown to be effective at increasing the uptake in breast cancer[17]. This study aims to use PEG to replicate the properties seen in breast cancer within human oral squamous cell carcinoma.

Reducing barriers to enter the cell stems from the nanoparticle's ability to selectively bind to cancerous cells. In addition to PEG, ligand used was cysteine modified peptide with a specific amino acid chain, RGD (arginine-glycine-aspartic acid) sequence peptide)[15]. For the purposes of this study, the RGD ligand a targeting ligand which allows it to bind to cancer cells as it is used to target a common cancer marker that is expressed in the membrane of many different cancer lines including human oral squamous cell carcinoma. The binding to this membrane allows for the uptake of the nanoparticle into the cell by endocytosis. This also adds selectivity to the nanoparticle as it binds only to the cancerous cells while leaving the healthy cells alone. Consequentially, photothermal treatment only causes apoptosis to the cancerous cells.

One of the most important aspects of nanoparticles is localization within the cell following uptake. The third ligand used in this study was a NLS (nuclear localization signaling) peptide . This ligand targets the nucleus by binding to the nuclear transport receptors[15]. One important aspect that allows for increased responses to photothermal treatment is the accumulation of nanoparticles within one specific area of the cell. The accumulation around the nucleus is important as nucleus damage bypasses many other pathways to initiate apoptosis. This study analyzes the potential application of NLS as a means of accumulation within the cell.

One of the main differences between the nanospheres and nanocubes is the surface charge. Different synthesis processes lead to different shapes occurring which also change the surface characteristics of the nanoparticle and in turn the surface charge. Nanoparticles with a negative surface are less likely to properly uptake[18]. These different ligands which are bound to the surface of the nanoparticle can have different effects on the charge associated with the surface and analyzed for a zeta potential, a measurement of surface charge. In nanoparticles, a zeta potential that lies between -10 and +10 mV is considered to be neutral while potentials that are greater than +30 mV or less than -30 mV are considered to be strongly cationic or anionic[19]. This associated charge can have a significant effect on the uptake of the nanoparticles along with their cytotoxicity. Throughout this study the zeta potential of the nanoparticles was analyzed to determine if the binding of different ligands cause a change in the surface charge. With an optimal goal to decrease the cytotoxicity of the nanoparticle to increase cellular uptake, how ligands effect surface charge plays an influential role in determining the ligands to use in this study.

Literature Review

Nanoparticles are materials that exist at the nanometer scale and can be engineered to have specialized compositions and functionalities[20]. Though these nanoparticles can have applications in many different fields, the emergence of the use of nanoparticles in biological and biomedical research has led to new forms of treatment and diagnostics. Nanoparticles may be synthesized from many different materials from liposomes to polymers to metals[20]. Some common metals used are gold or silver. The emergence of gold nanoparticles as one of the front runners in terms of medical nanoparticles has stemmed from their low toxicity combined with their large variety of optical properties[20]. Gold nanoparticles have been used in diagnostics, photothermal therapy, and as drug carriers[12]. This study focuses on the optimization of gold nanoparticles in human oral squamous cell carcinoma cells, human oral squamous cell carcinoma, for their implementation of photothermal therapy.

The use of nanoparticles as a means of local drug delivery has been explored for applications in cancer treatment. There are a variety of means by which a nanoparticle can be used to deliver drugs. One way is by synthesizing nanoparticles that experience structural changes such as the expansion of the shell given different pH environments[2]. When a nanoparticle moves from a neutral to acidic region a common characteristic for cancer microenvironments, the shell can expand and release the drug that was encapsulated. Another mode by which nanoparticles can be used to deliver drugs is through different coatings on the outside of the nanoparticle. By coating, the outside of the nanoparticle with the drug the nanoparticle can then be controlled to reach the intended location either through magnetic or thermal properties[21]. Though pH-controlled release

of drugs has shown promise this study chose to focus on the coating of the nanoparticle and using the nanoparticle itself as a therapeutic.

Despite the progress that has been made, one of the main struggles that face the future of nanoparticles as a means of cancer treatment is the optimization that is required for each type of cancer. As each different type of cancer cell differs not only structurally but also mechanistically, each nanoparticle must be specially tailored to the type of cell it is intended for. Though this study requires the optimization of the nanoparticle to be tailored to the specific type of cancer, the overall form of treatment, photothermal therapy, can be applied to cancers that are not in deep tissue. One of the biggest differences stems from the uptake of the nanoparticles into the cells which can be optimized to take advantage of the mechanisms already present in a specific cell type.

The conjugation of different ligands to the exterior of nanoparticles helps to overcome the biological barrier and allows a foreign object into the cells while using the cell's mechanisms to its advantage. Bellis has shown that in the past the use of RGD peptides can be used to enhance the cell biomaterial interaction[22]. The binding of RGD to the exterior of biomaterials has been shown to increase the adhesion of the biomaterial to the cell[22]. This predicts that the conjugation of RGD to the exterior of gold nanoparticles can lead to the nanoparticles being able to adhere to the cells. This study aims to show that the binding of RGD to the exterior of the nanoparticle allows for uptake into human oral squamous cell carcinoma cells despite it has not been previously shown that the binding of RGD to a nanoparticle leads to uptake of nanoparticles specifically within human oral squamous cell carcinoma cells they over express a cancer marker that RGD binds to.

Though RGD allows the nanoparticle to bind to the cell, it does not decrease the cytotoxicity of the nanoparticle. Shenoy analyzes another substrate, polyethylene glycol, PEG, and its ability to increase cell-biomaterial interacions[17]. The conjugation of PEG has been shown to decrease cytotoxicity and as a result, allows for longer-term circulation of nanoparticles[17]. Not only does this decreased cytotoxicity enhance cellular uptake, but Panikkanvalappil has also shown that they can increase the uptake of the nanoparticles through receptor-mediated endocytosis[23]. This facilitated uptake takes advantage of receptors already present on the cells while also decreasing the chances of rejection. This study takes advantage of these shown properties by binding RGD to the exterior of the nanoparticle in combination with PEG.

Furthermore, the use of nuclear localization signaling peptides, NLS, as a means of directing the nanoparticle to the nucleus once it has been up taken into the cell has also been examined[23]. By directing the nanoparticle to the nucleus, it helps to allow a faster localization of nanoparticles. This localization around the nucleus helps to increase a concentrated drug delivery, which oftentimes is focused on attacking the nucleus. This study takes the localization as driven by NLS and applies it to photothermal therapies. By bringing the nanoparticles together it allows them to have more of an effect when heating up than they would scattered throughout the cell.

One of the main disadvantages of common chemotherapeutic treatments is the ability to develop resistance to the drug. One of the most common chemotherapeutics, cisplatin, attacks cancerous cells through multiple pathways at once[24]. This allows it to be an effective treatment for several types of cancers, however, due to its multipronged approach, the changes a cell undergoes when developing resistance are not well understood. A pathway to overcoming resistance would allow

for more effective treatment of additional cancers. This study aims to provide that pathway by combining nanoparticle and cisplatin treatment simultaneously.

This study looks at the applications of nanoparticles and their ability to help overcome cisplatin resistance. Optimization of the nanoparticles for human oral squamous cell carcinoma cells occurred using RGD, PEG, and NLS in different ratios to determine the ratio that leads to the maximum uptake. With the use of this optimized nanoparticle, the effect that cisplatin resistance has on the uptake of nanoparticles was studied. Understanding the difference in uptake from non-resistant to resistant cells can help to lead to a better understanding of the effects that cisplatin resistance has on cell membrane receptors and transport. If this approach is proven to overcome cisplatin resistance, this approach may be able to be expanded to other cancers. This would be able to lead to an increased treatment success rate for second or third cancer occurrences.

Methodology

Synthesis of Nanocubes

The optimization of nanocubes was studied to find the optimal concentrations of various components necessary to form a nanocube conducive to uptake within the cell while also having proper light scattering properties. The cubes were created by initially combining H_2O (40 mL) with cetyl trimethylammonium bromide, CTAB, (8000 µL, 0.1 M) and ascorbic acid (6000 µL, 0.1 M). The final ingredient sodium borohydride (1 mM) was added in various volumes (2 µL, 5 µL, 20 µL, 40 µL) which lead to changes in the overall size of the nanoparticle. The absorption spectra were obtained of each of the different solutions at various times after the addition of the sodium borohydride to study the rate of synthesis while also studying size changes. Following the completion of this study the nanocubes were made by combining H_2O (40 mL), cetyl trimethylammonium bromide, CTAB, (8000 µL, 0.1 M), ascorbic acid (6000 µL,0 .1 M) and sodium borohydride (20 µL, 1 mM)[25].

Synthesis of Nanospheres

The synthesis of nanospheres was done to form nanospheres of a viable size for imaging, trying to create nanospheres that allowed for optimal uptake but were not too small for accurate imaging. Initially Au (3.75 ml, 10 mM) was added into H_2O (135 mL) and brought to a boil. Once the solution comes to a boil the trisodiumcitrate (5 mL ,35%) was added in causing the solution to complete a color change from a dark purple to a deep red wine color. The amount of trisodiumcitrate controls the overall size of the nanospheres with more trisodiumcitrate leading to a smaller particle. Nanospheres produce peaks in the 520-530 nm region[25].

Conjugation of Nanoparticles

The nanoparticle itself does not readily uptake into the cells and must therefore be conjugated with different ligands to help achieve uptake. One ligand is Polyethylene glycol (PEG), an ethyl functionalized polymer that allows binding by forming a covalent bond to create a thiol bond which comes in many different lengths and serves to protect the molecule and make it cell viable. Another ligand that was used was arginine-glycine-aspartate, RGD, a tri amino acid sequence adhesive peptide that helps to provide a bio-tolerant surface throughout endocytosis. Additionally, it helps to bind to the targeted proteins while also binding to the nanoparticles in controlled densities. The third ligand is a nuclear localization sequence, NLS, is an amino acid sequence which can be used to assist with uptake and endocytosis by binding to the nuclear membrane and serving as a nuclear transport facilitator. Nanospheres and nanocubes were bound with vary percentages (100% PEG, 50% PEG/ 50% RGD, and 50% PEG/ 30% RGD/ 20% NLS) of the three ligands to study the varying effect on uptake. These nanoparticles were conjugated by exposing the particles to the correct about of ligand necessary given the size, shape, and concentration of particles. The nanoparticles are then allowed 24 hours for complete conjugation before use in any study[26].

Cell Preparation

For different experiments either breast cancer, MDA-MB-231 or human oral squamous cell carcinoma, HSC-3 cell lines were prepared. Both non-resistant and cisplatin resistant cells were cultured. The cells were first split and then later injected with the different nanoparticle solution. The cells were taken from a plate on which they were previously split. The media was pulled from the plate. The plate was then rinsed with PBS to stabilize pH and remove dead cells. The PBS was then removed. Trypsin (1.5 mL) was then added to the plate to release the cells from the plate. The

plate was then incubated (5-7 min). More new media (1.5 mL) was added to the plates once the cells had released fully to neutralize the remaining trypsin. The entire solution was then removed and placed into a vial and centrifuged (5 min 1500 RPM). The old media is discarded leaving the pellet. New media is added to the vial. Media (10 mL) is added to a new plate. Some of the new pellet and media solution is added to the plate for later cell line splits[27]. For experiments involving cisplatin resistant cells, 24 hours after initial splitting of cells cisplatin (20 uL, 5.4 uM) was added to the plate. The media was replaced 24 hours later to allow for the growth of the resistant cells. Cells that were more resistant to the cisplatin required longer incubation period so after two rounds of treatment the incubation period before exposure to cisplatin was increased to 48 hours. For experiments involving dark field imagining, cover slips for every reaction, a control and the three different solutions with various ligands, were each placed into a well plate. Some of the media and pellet solution was added into each well to dilute the cells to the proper level. Cells were then incubated for 24 hours before being injected with the proper ligand solution. Cells were then incubated for 24 hours. This was repeated for both cell lines with all solutions using both nanocubes and nanospheres.

Cell Analysis using Dark Field Imaging

Dark field imagining allows for images of the cells to be taken by using the light scattering properties of the nanoparticles. Images of the cells were taken once the cells had undergone nanoparticle uptake for 24 hours. The cover slips from the well plate were then used to create slides for each of the different runs. If the run has nanoparticles, all except the control, the slides are first rinsed with PBS and then added to media again. The coverslip was removed from the well and placed on the slide plate. Media (650 μL) was then added to the slide plate. Slide was placed into

the incubator until ready to measure it under the microscope. The slide was then analyzed using a Leica Infinity 2 microscope[26].

Image Analysis for Optimization of Nanoparticles via Uptake Studies

The images obtained from each run were then analyzed in ImageJ Fiji to calculate the intensity which can be used to determine the uptake of the nanoparticles into the cells. The images from five different sections of the field were chose and analyzed. The intensity is proportional to the amount of uptake that occurred as more uptake leads to more scattering and in turn a more intense response. The image was upload into ImageJ and converted from a 32-bit RGB image to a 16-bit grayscale image and in turn to a binary reading. This binary reading allows for the intensity of individual cells to be tracked. For each run the average intensities for each cell were then used to find an average intensity for the uptake for a given run.

Cell Analysis and Drug Introduction

Both HSC-3 and MDA-MB-231 cells obtained from ATCC were cultured and analyzed for cell movement. After exposure to nanoparticles, the cells were then monitored to study the movement both in the case of exposure to Cisplatin and without Cisplatin. Each well was place into an Olympus IX70 Inverted Microscope to allow for constant pictures to be obtained of the movement. In the microscope the conditions were carefully maintained throughout the whole run time. The temperature was maintained by running water around the well at a constant temperature. The environment was also maintained by the constant presence in both flow and pressure of carbon dioxide. Cisplatin of various concentrations were added to the cells. An image of the cells was then obtained every two minutes with a Nikon camera. These images were set to automatically be

captured to ensure constant and consistent timing. This allowed for a real time analysis of the Cisplatin interaction with the cells.

Movement Analysis of Cisplatin Exposed Cells

The images that were obtained from each run were then compiled into a video. This video had each photo as a new frame allowing for the position and velocity to be tracked over time. The video was then uploaded into ImageJ for processing. ImageJ was used to track the movement of individual cells across the entirety of the time. Every individual cell was followed throughout the duration of the video. Once the single cell had been tracked the track was ended. This was repeated with the other cells visible in the frame, adding a new track for each new cell. The data collected was then added into Excel. This data was used to plot the position of each cell over time. The position of each cell was reoriented to show all the position paths at the same time. The position data was then used to generate the velocity for each of the cells. The average velocity was then calculated for each different exposure to Cisplatin

Zeta Potential and Hydro Dynamic Light Scattering

Zeta potential and hydro dynamic light scattering testing was done on the conjugated nanoparticles to determine the surface charges along with the size of the nanoparticles. This analysis shows the changes that the different conjugations had on both the overall size of the particle and the surface charge which can lead to changes in uptake. The conjugated nanoparticles were centrifuged lightly. After centrifuge the nanoparticles (500 uL) were added to the DIP Cell. The DIP Cell was inserted into the Malvern Zetasizer Nano Series and the sample was run. The zeta potential was then graphed versus the number of times it occurred. From this an average zeta potential was calculated.

Each different conjugation was run in triplicate[28]. The conjugated nanoparticles were also run in a Wyatt DynaPro NanoStar to determine the radius via dynamic light scattering. The nanoparticles (200 uL) were added into the cuvette and placed into the NanoStar and run at constant temperature (25 C). The average radius was then graphed versus intensity for different conjugations. Each different conjugation was run in triplicate[29].

Cell Analysis via Cell Viability

Cell analysis was performed via a Vi-CELL cell viability assay. The viability assays were used to determine the survival rate of the HSC-3 cells under a variety of conditions to determine whether the nanoparticles themselves had an inherent toxicity of the cells. The viability was tested for each of the cell lines. The viability was run for just the cell, the cell in the presence of cisplatin, the cell in the presence of the nanoparticle, and the cell in the presence of cisplatin and the nanoparticle.

Results and Discussion

The physical characteristics of the nanoparticles used lead to light scattering, which can be observed through different forms of microscopy. Analyzing nanoparticles through microscopy allows for easy assessment to assure that the intended processes are occurring, and that the nanoparticles are being delivered to the cells. Throughout this study, the imaging properties of the nanoparticles were used to quantify the cellular uptake. The light-scattering properties of the gold nanoparticles were combined with dark-field imaging to get an accurate portrayal of uptake and localization with HSC-3 cells in this study.

Analysis of the effect of Sodium Borohydride on Growth of Nanocubes

The creation of nanocubes was studied to find the correct concentrations of various ingredients necessary to form an effective nanocube. The cubes were created by initially adding H_2O (40 mL) with cetyl trimethylammonium bromide, CTAB, (8000 µL,0.1 M). Next ascorbic acid (6000 µL, 0.1 M) was added. The final ingredient sodium borohydride (1 mM) was added in various volumes (2 µL, 5 µL, 20 µL, 40 µL). The absorption spectra were obtained of each of the different solutions at various times after the addition of the sodium borohydride ($NaBH_4$).

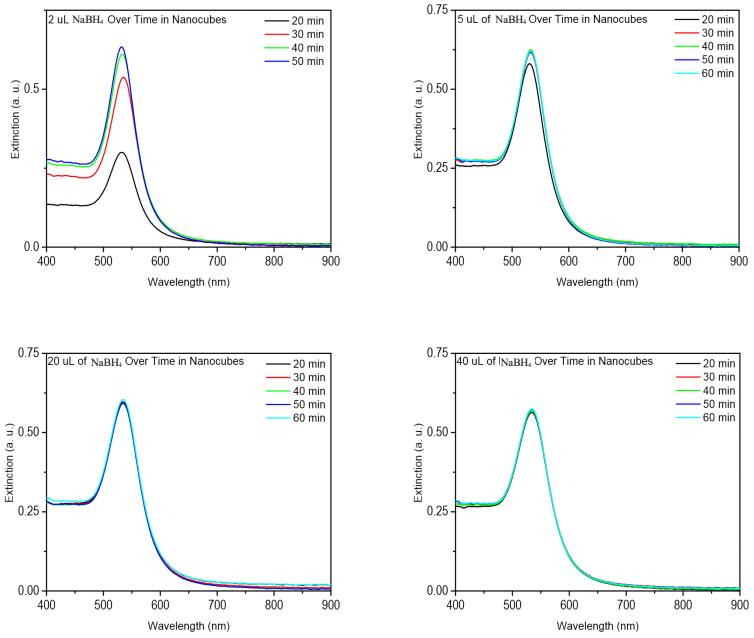

Figure 1. *Wavelength comparison of cubes created with various concentrations of sodium borohydride over time.*

This impact of the amount of $NaBH_4$ on the growth rate of the nanoparticle is visibile only in the solution with 2 uL (figure 1). This is because in the other solutions the concentration of the $NaBH_4$ is so high that the reaction runs almost immediately to completion. In the 5 µL $NaBH_4$ solution there is a visible shift between the 20-minute solution and the others. This shows that after 20 minutes the solution was still not at completion. This comparison over time reinforces the fact that the nanocubes should not be immediately used if created with a low volume of $NaBH_4$ while also showing that the addition of $NaBH_4$ is only a limiting factor in low concentrations.

Synthesis of Nanocubes

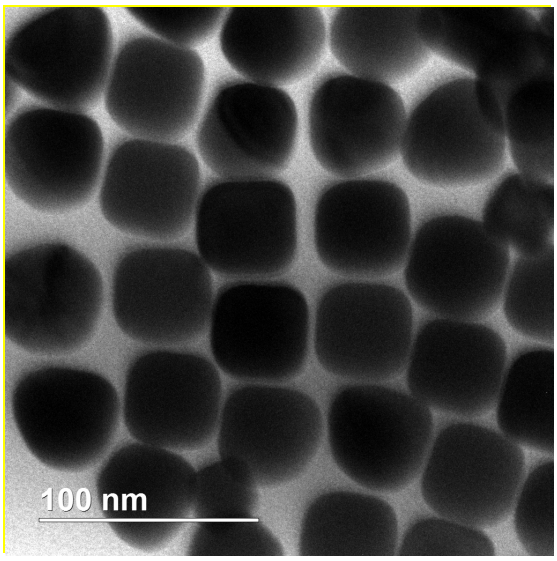

Figure 2. *Image of the nanocubes used in the experiment along with the correct scale.*

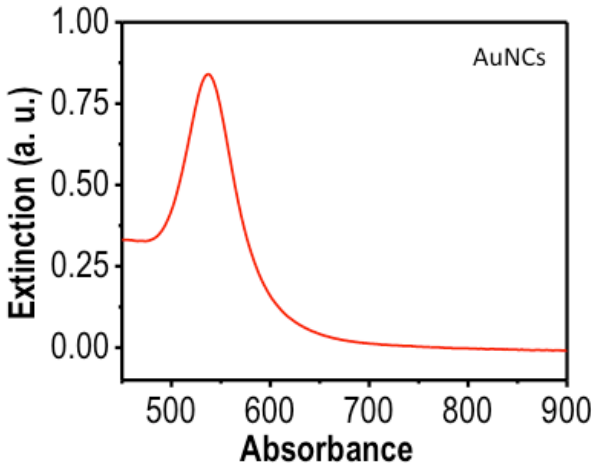

Figure 3. *Absorption spectrum of the nanocubes used in this experiment.*

Uptake of Nanocubes in MDA and HSC

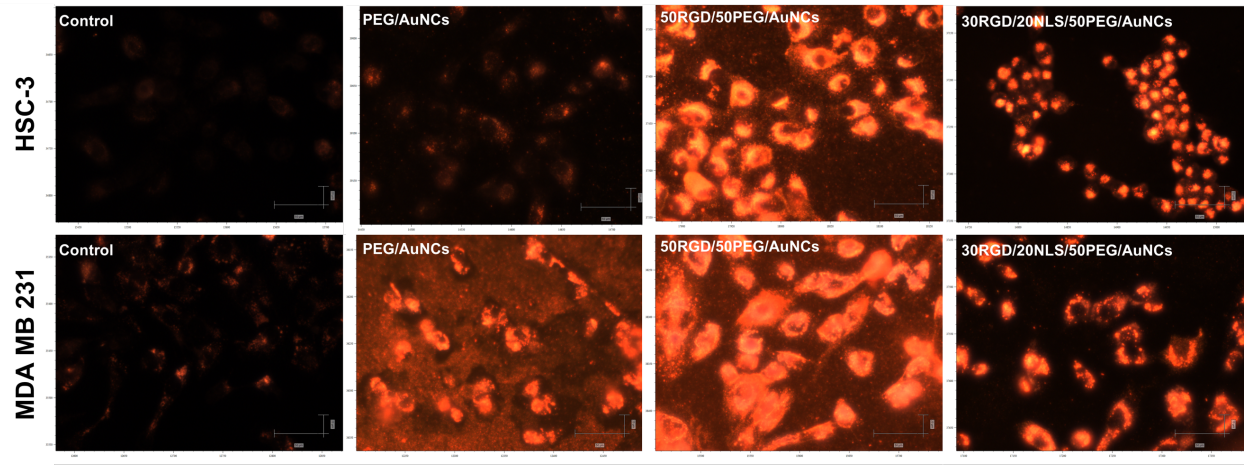

Figure 3. *Uptake of Nanocubes bound with different ratio of ligands in HSC-3 and MDA-MB-231*

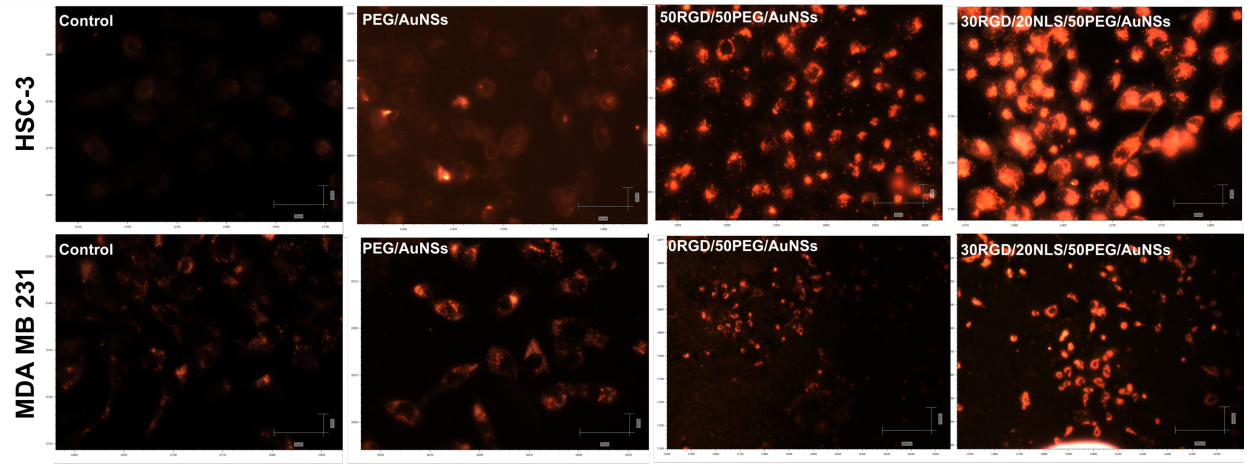

Figure 4. *Uptake of Nanospheres bound with different ratio of ligands in HSC-3 and MDA-MB-231*

Absolute Intensity Comparison

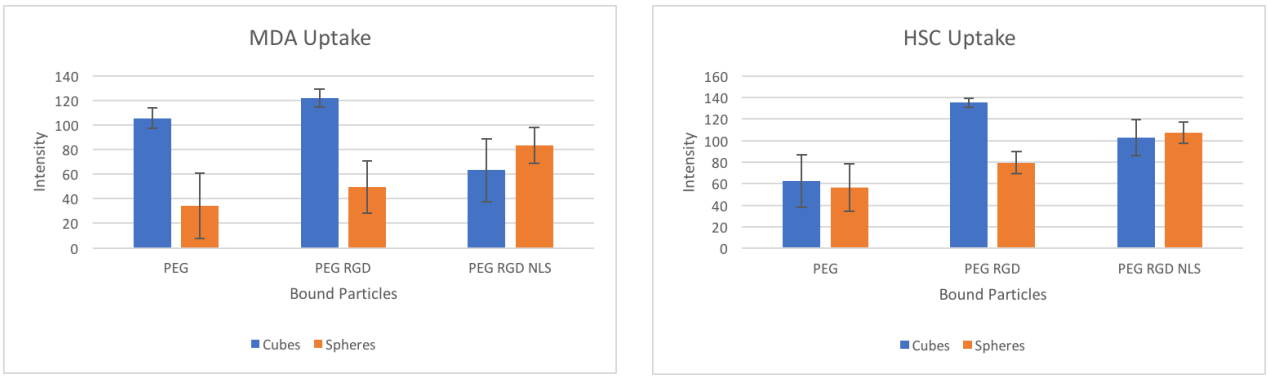

Figure 5. *The absolute intensities for the uptake of the ligands with different bindings calculated for both MDA-MB-231 and HSC-3.*

The absolute intensity of the uptake was measured for both cell lines, MDA-MB-231 and HSC-3, with particles bound with PEG, PEG and RGD, and PEG RGD and NLS (figure 6). The intensities were measured using ImageJ. The uptake images were converted to grayscale images and the brightness from the cells were then measured. The cells were exposed to both the nanocube and the nanosphere shapes to assess if the trend were shape specific. In both cell lines, there was a similar trend for the intensities of the cubes. For both the PEG and RGD bound nanocubes experience the most uptake while both the PEG RGD NLS bound along with the only PEG bound experienced much less uptake. Both cell lines also experienced similar trends with the ligand

bound spheres. The PEG only bound particles experienced the least uptake while the PED RGD and NLS bound particles received the most uptake. The data was analyzed using ANOVA. The F value was 312.73 with a p value that is less than .00001 indicating that the results are significant at $p<.05$. The difference in the two trends is due to a change in the surface charge associated with a change in surface area and number of ligands which can bind.

Understanding the best ligands to bind to different nanoparticles and understanding how a specific cell line will react to the change in ligands allows for a more specific and targeted nanoparticle to be used on the cell line. By varying the type of nanoparticle that was used the uptake intensity that was experienced was drastically different. This is due to a change in surface charge based on how it is made and may be explained by the CTAB potential. The nanocubes were made with CTAB, which can cause a cationic surface on the nanocubes. Ideally nanoparticles would have no surface charge as a surface charge can lead to cytotoxicity. The difference in the surface charge of the nanocubes and nanospheres could explain the difference in the uptake trends. This charge could have led to additional matrix effects, which caused the PEG RGD and NLS bound nanocubes to have less uptake which is not what was expected. The nanospheres on the other hand increased the uptake with the addition of a ligand. This is more like what was expected. Though the general trends were the same the HSC-3 cells experienced more uptake. This was analyzed through a one-tailed to test to determine the p value of .0038 which indicates that the increase is statistically significant. Though the nanocubes bound with PEG and RGD had the most uptake the fact that adding in the additional ligand lead to a decrease appears to have an additional underlying factor.

Movement of HSC-3 Cells

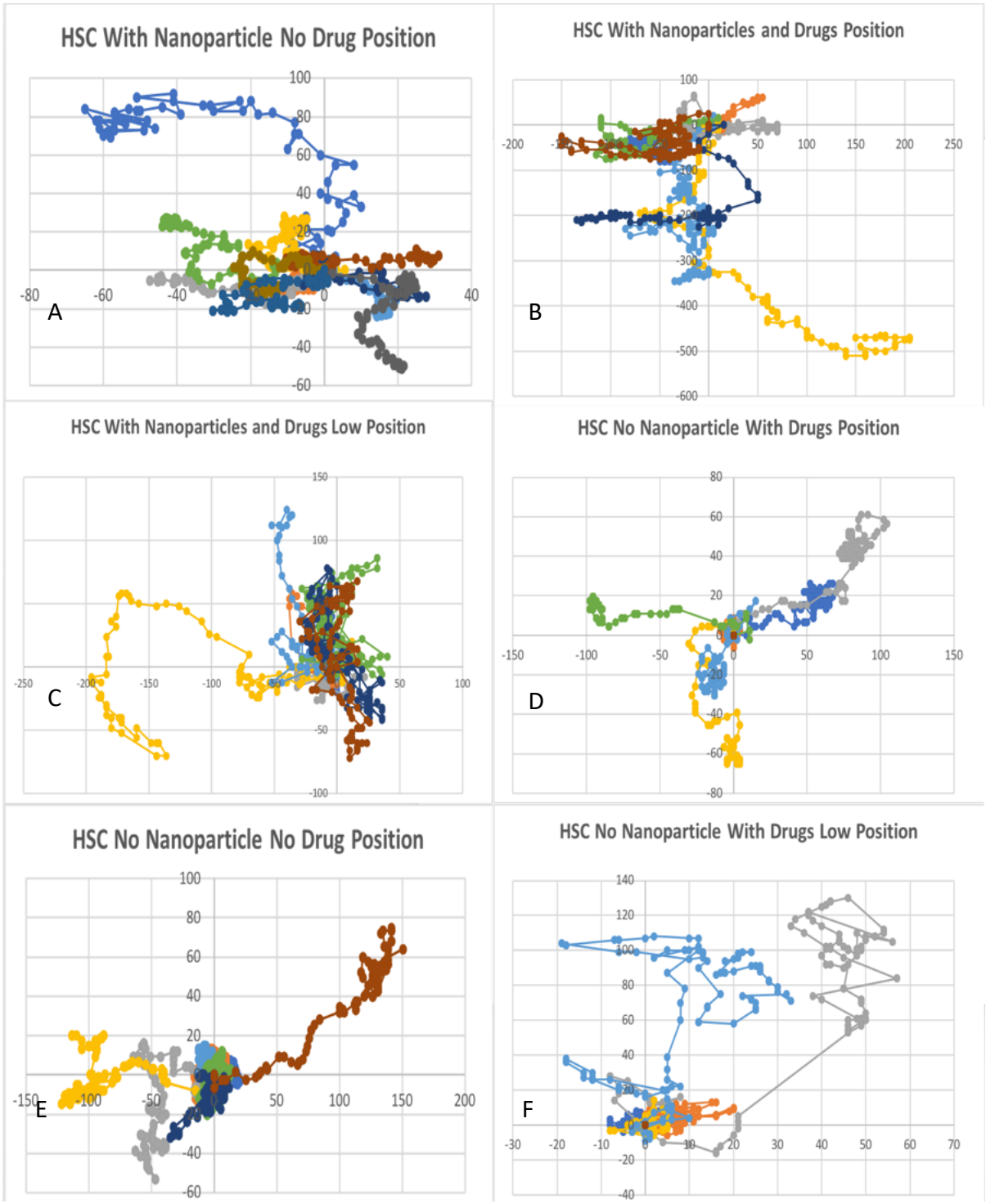

Figure 6. *15 cells were track for each study. A: HSC cells with nanoparticles without the cisplatin position. B: HSC cells with nanoparticles and cisplatin at a low concentration position. C: HSC cells with nanoparticles and cisplatin at a low concentration position. D: HSC cells without nanoparticles and with a low concentration of cisplatin position. E: HSC cells without nanoparticles or cisplatin position. F: HSC cells without nanoparticles with a low concentration of cisplatin position. The position of all the different cells is measured in um.*

Not only were still images of the HSC-3 cells with nanoparticles obtained, but also live videos were obtained which allowed the movement of the cells to be studied. This analysis allowed for an assessment on the impact that the addition of nanoparticles has on metastasis. This additional functionalization allows the nanoparticles to be utilized beyond a curative treatment, attacking the present illness, but also preventative, reducing the chance of the cancer spreading. The HSC with nanoparticles in the presence of a high concentration moved significantly more than the HSC without the cisplatin with a p value of .0021 (figure 7B). This indicates that the presence of cisplatin increases the mobility of the HSC cells. The HSC with the nanoparticles and a low concentration of cisplatin moved similar distances as compared to the HSC with nanoparticles without cisplatin (figure 7C). While the mobility was increased, it was not done to the same degree as it was in the higher concentration with a p value of .037. This indicates that the higher the concentration of cisplatin the more the mobility is increased. The HSC without the nanoparticles or the cisplatin moved slightly more than the HSC with the nanoparticles (figure 7E). This appears to indicate that the addition of nanoparticles decreases the mobility of the cells. This reaffirms the belief that nanoparticles used as a means of treatment have the potential to reduce metastasis on their own.

Table 1. *Average Velocity of HSC Cells Per Hour*

	Hour	Nanoparticles with Drug High Concentration	Nanoparticles with Drug Low Concentration	Nanoparticles without Drug	No Nanoparticles or Drugs	No Nanoparticles with High Drug Concentration	No Nanoparticles with Low Drug Concentration
	1	0.563	1.94	0.925	2.73	1.46	1.57
	2	0.441	1.60	0.925	2.73	0.753	1.43
	3	0.319	1.26	0.925	2.73	0.346	0.876
	4	0.197	0.918	0.925	2.73	0.124	0.765
Avg.		0.380	1.43	0.925	2.73	0.671	1.16

The average velocity of the different runs was analyzed every hour (table 1). When not in the presence of drugs the velocity was steady throughout the duration. The HSC-3 cells with the nanoparticles had a much lower velocity than that of the HSC-3 cells without the nanoparticles as concluded by a t test with a p value of .025. This indicates that the presence of the nanoparticles along decreases the velocity as seen by the decreased movement (figure 7). The HSC cells with nanoparticles with the higher concentration experienced a much lower average velocity than that of the lower concentration. Both runs however experienced an over 50% decrease in velocity by the end of 4 hours. The average velocity for the low concentration was however over 3 times as high as that of the high concentration. A similar pattern was observed in the HSC cells without the nanoparticles. The average velocity for the low concentration was twice as high as that of the high concentration. This indicates that the increase in the concentration of the cisplatin leads to a greater decrease in velocity.

Cell Viability Analysis

Table 2. *The cell viability was run for every line for the cell alone, in the presence of cisplatin, in the presence of nanoparticles, and in the presence of cisplatin and nanoparticles.*

Name	Doses	Cell Alone	Cell in the Presence of Cisplatin	Cell in the Presence of Nanoparticles	Cell in the Presence of Nanoparticles and Cisplatin
Control	0 doses	100.00	69.78	133.81	68.73
Round 4	1 dose	100.00	85.85	148.20	126.01
Round 3-1	2 doses	100.00	79.02	108.60	70.64
Round 3-2	2 doses	100.00	78.47	88.43	81.61
Round 2-1	3 doses	100.00	84.05	88.95	89.39

The viability of the cells in different combinations of cisplatin and nanoparticles leads to different results in cell viability (table 2). The viability is indicative of the response to the cisplatin or to the nanoparticles. Different trends can be analyzed based on the number of doses

of cisplatin that were used to create the cell line. These trends were then compared to the control which had no prior exposure to cisplatin. Though not enough data was obtained preliminary data was used to draw potential conclusions.

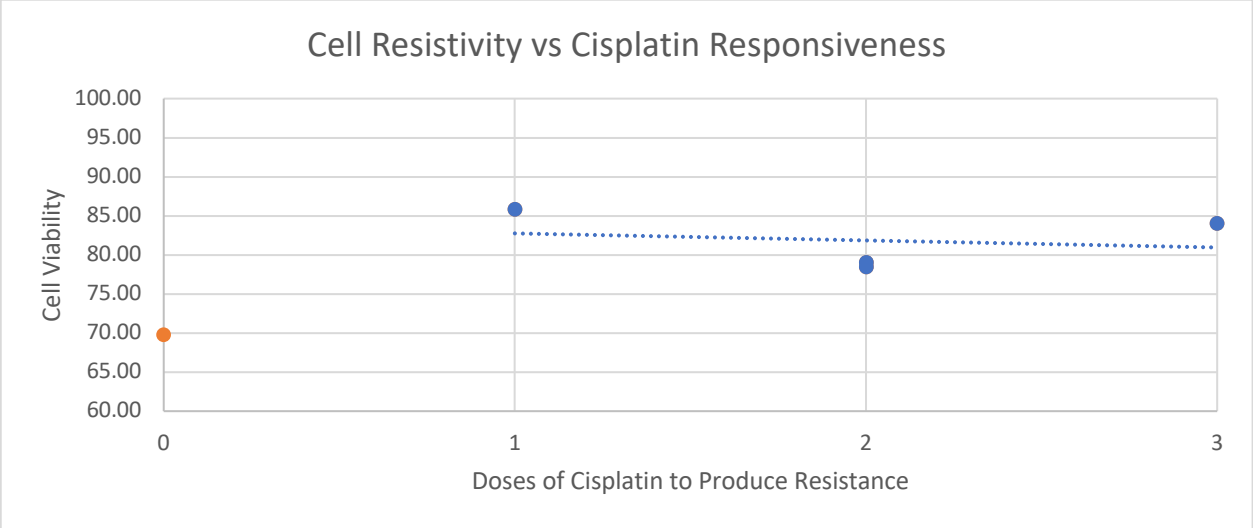

Figure 7. *The cell viability was measured for the cell in the presence of cisplatin alone over all cell lines. The control, with no doses of cisplatin is shown at 0. The cell with one treatment of cisplatin is show at one. The cells with two separate doses of cisplatin are shown at two. The cell with three doses of cisplatin are shown at 3.*

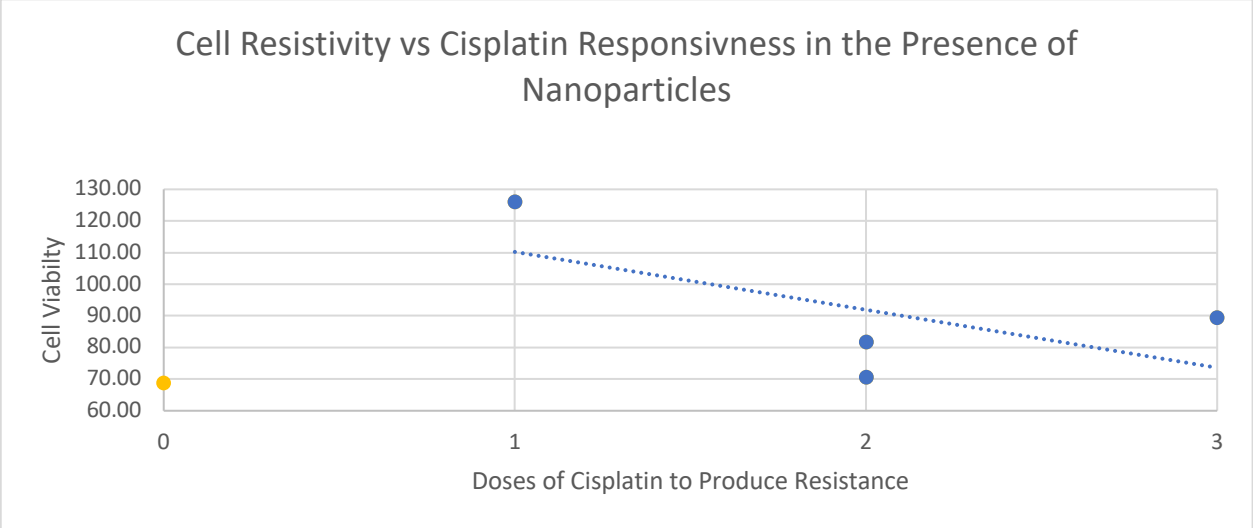

Figure 8. *The cell viability was measured for the cell in the presence of cisplatin and treated with nanoparticles. The control, with no doses of cisplatin is shown at 0. The cell with one treatment of cisplatin is show at one. The cells with two separate doses of cisplatin are shown at two. The cell with three doses of cisplatin are shown at 3.*

Cell resistivity due to previous doses of cisplatin lead to a much higher cell viability than that of the control cell which had no previous exposure (figure 8). The cell with only one previous does

of cisplatin to produce resistance had the highest cell viability and in turn the highest resistivity. The cell viability can be seen to remain steady the more that the cell was exposed to cisplatin. This is indicative of prolonged and repeated exposure to cisplatin reducing the resistance. However, the control with no previous exposure had the lowest cell viability. It is projected that the amount of prior exposure to cisplatin does not dramatically change the resistivity. A different pattern can be seen in the presence of nanoparticles (figure 9). Though the cell viability is drastically higher for those treated with nanoparticles, the cell viability also decreases rapidly. It can even be seen that the cell viability of the control is only marginally lower than that of the cells treated with cisplatin two times previously. This indicates that the presence of nanoparticles can cause a dramatic change in the cell viability while the trend remains the same whether nanoparticles are present or not.

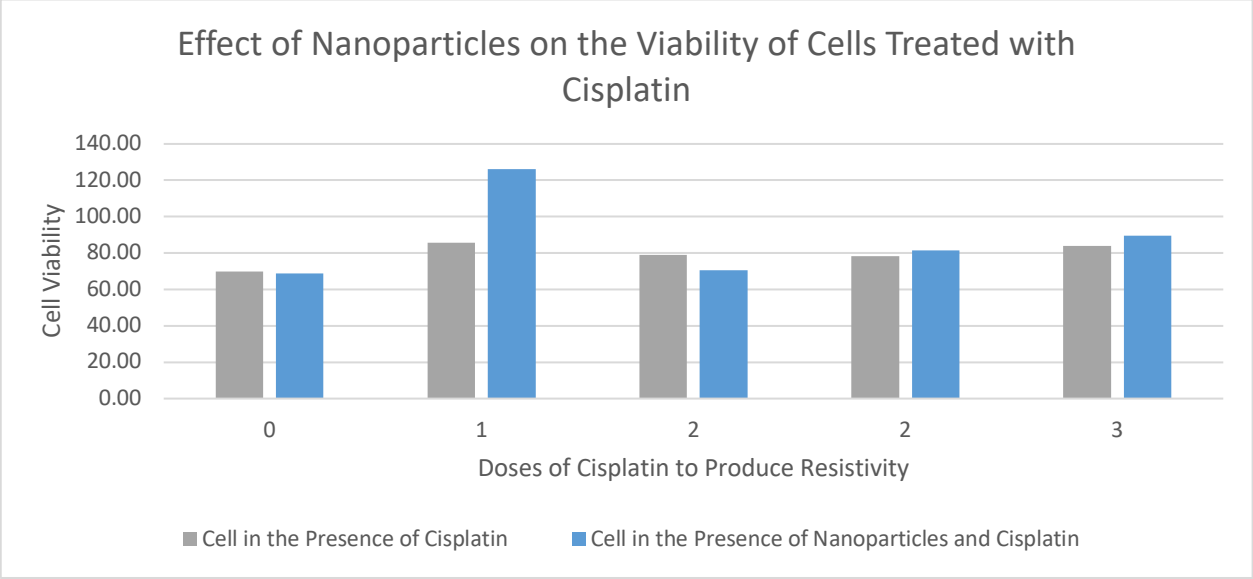

Figure 9. *The viability of the cells that were treated with cisplatin were compared to those that were also treated with nanoparticles. The control, with no doses of cisplatin is shown at 0. The cell with one treatment of cisplatin is show at one. The cells with two separate doses of cisplatin are shown at two. The cell with three doses of cisplatin are shown at 3.*

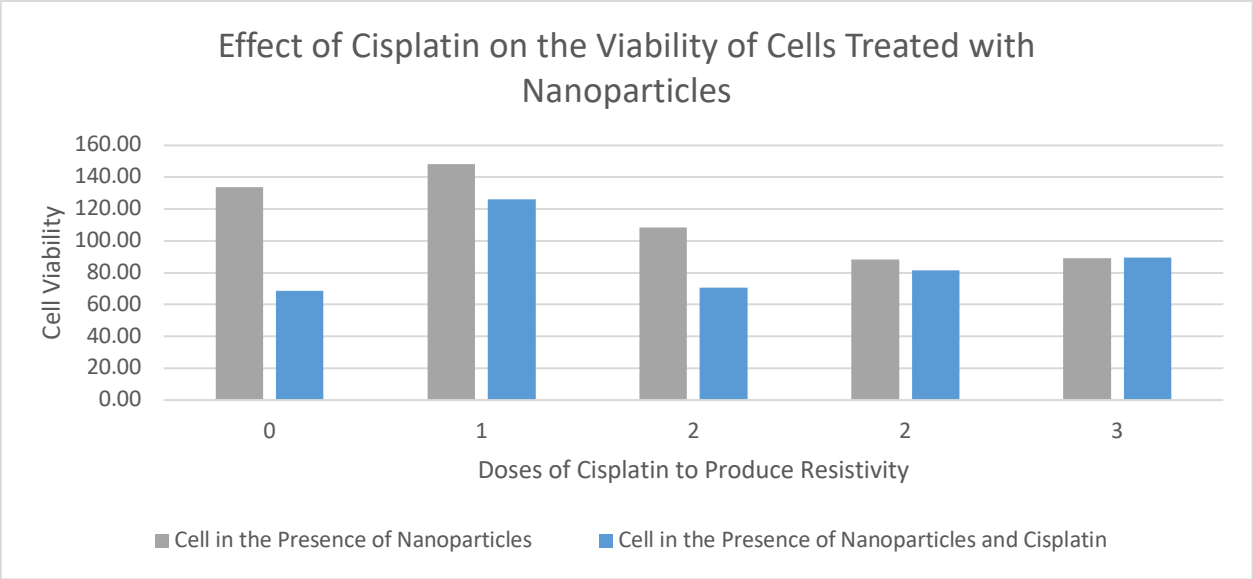

Figure 10. *The cell viability of cells in the presence of nanoparticles was compared to those in the presence of nanoparticles and cisplatin. The control, with no doses of cisplatin is shown at 0. The cell with one treatment of cisplatin is show at one. The cells with two separate doses of cisplatin are shown at two. The cell with three doses of cisplatin are shown at 3.*

The presence of nanoparticles is preliminarily believed to not have an effect on the cell viability of the control cells (figure 10). This indicates that the nanoparticle has a low toxicity on the cell. The only toxicity and harm to the cell as a result is coming from the presence of cisplatin and not from the nanoparticle itself. This is an encouraging as if nanoparticles pose no innate harm or distress to the cell, they will not cause any harm or distress to a normal healthy cell which could allow them to be used as a form of treatment. It is shown that the presence of nanoparticles leads to a higher viability, though that initial increase is lessened over time. The difference between those cells in the presence of nanoparticles which were treated with cisplatin is also lessened over time (figure 11). The fewer the number of prior doses of cisplatin the greater the difference in cell viability between those treated with cisplatin and those not in the presence of nanoparticles.

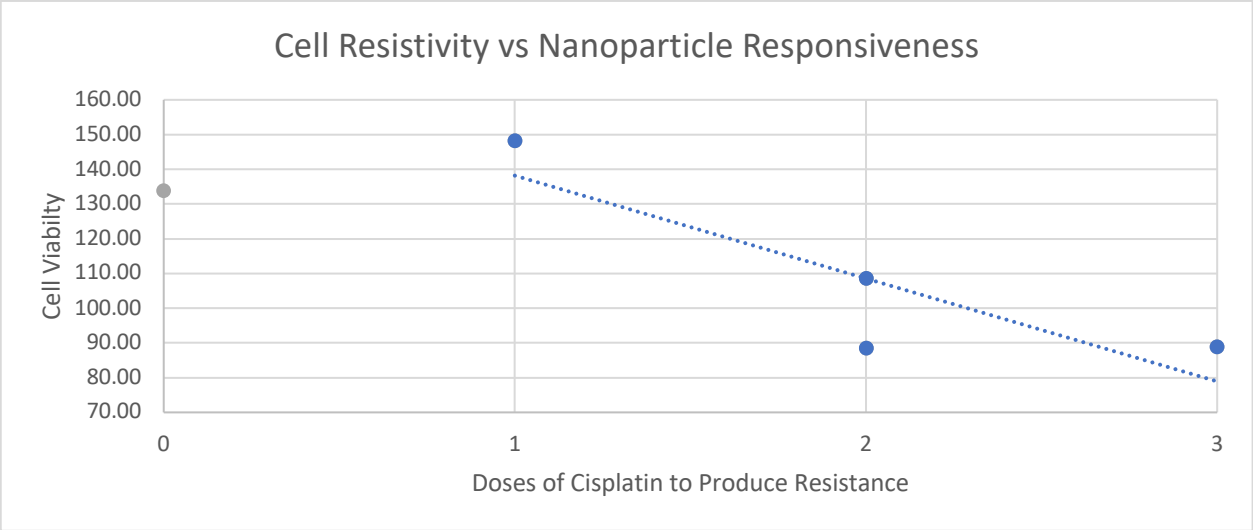

Figure 11. *Each of the cells were treated with nanoparticles and the cell viability was run. The control, with no doses of cisplatin is shown at 0. The cell with one treatment of cisplatin is show at one. The cells with two separate doses of cisplatin are shown at two. The cell with three doses of cisplatin are shown at 3.*

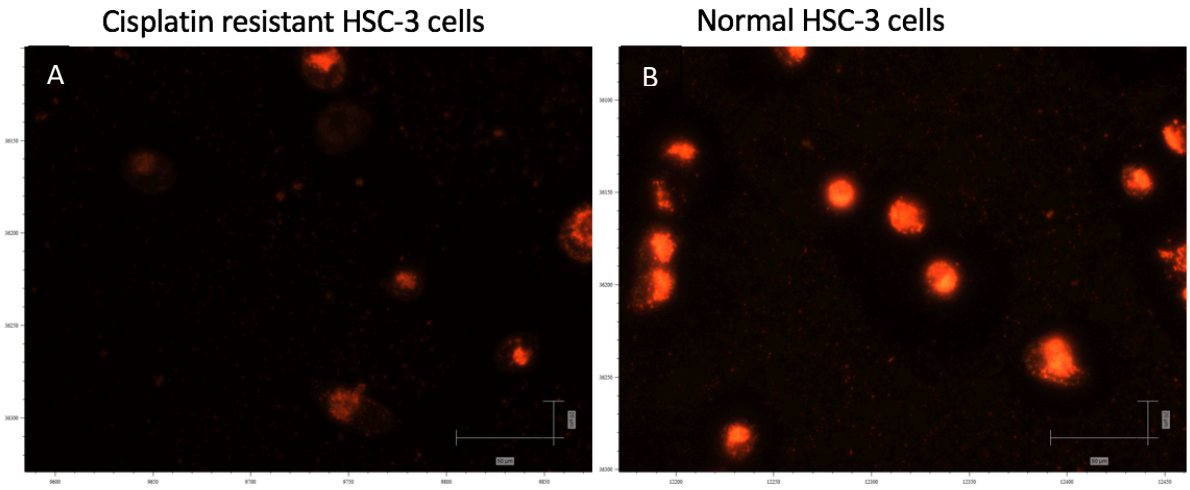

Figure 12. *The uptake of nanoparticles by both a resistant cell and a nonresistant cell was analyzed by dark field imaging. A: The uptake of nanoparticles in cisplatin resistant HSC cells that received 3 separate doses of cisplatin. B: The uptake of nanoparticles in normal non-treated HSC cells.*

When treated with nanoparticles but not cisplatin the cell viability initially increases (figure 12). With more than one prior does of cisplatin, however the cell viability decreases drastically. This could be due to a lesser uptake of nanoparticles by cells with more previous doses of cisplatin (figure 13). The more doses of cisplatin that a cell received the more that it changed the cell itself. The more treated cells would require and inoculation time that was between two to three

times as long as a normal cell to reach the same level of confluency. The shape of the treated cells also started to differ slightly from that of normal cells. These changes indicate that the growth pattern, along with the structure of the cells is impacted by treatment with cisplatin. The difference in the structure could lead to differences on the surface which impact nanoparticle uptake. It is possible that this lower uptake is the cause of the decrease in cell viability as the number of previous doses of cisplatin increases. The only cell with higher viability is that which was only treated with cisplatin once prior and had a much faster growth rate and fewer visible differences. If the nanoparticle was to be adopted to allow for better uptake into the more dosed cells it could dramatically increase the cell viability as seen in the cell with only one prior dose of cisplatin (figure 10). The connection between nanoparticle uptake and the cell viability is strong (figure 11). With a greater uptake in nanoparticles the cells which received more prior doses of cisplatin would in turn have higher viability.

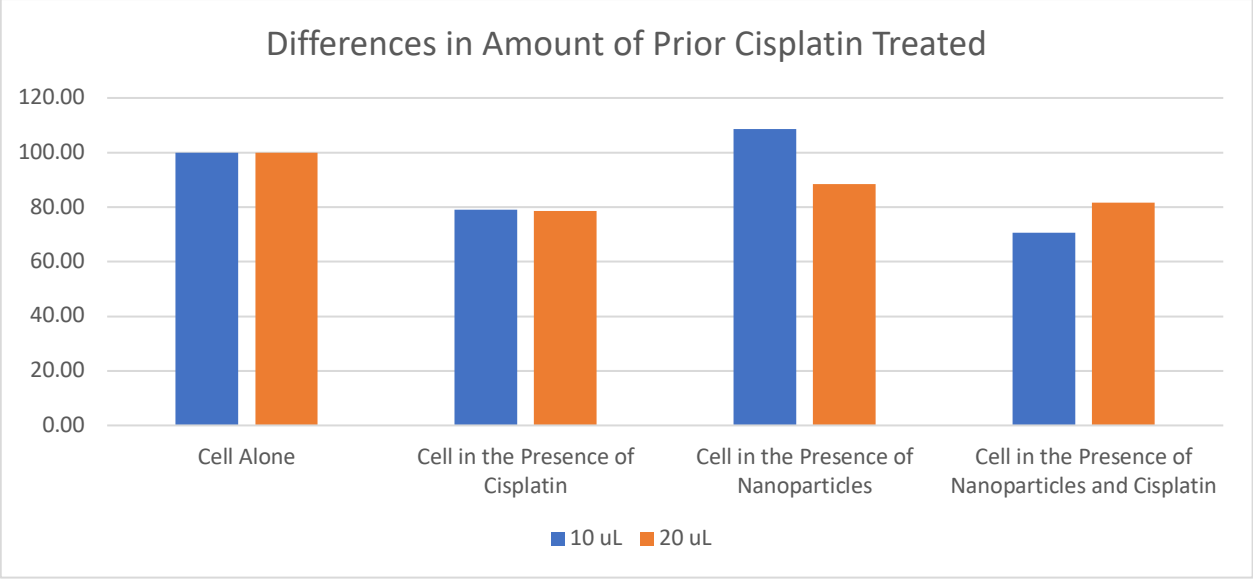

Figure 13. *Two cells which received the same number of prior doses of cisplatin received different amounts of cisplatin each time.*

For the two cells which underwent the same number of previous doses of cisplatin, but different amounts each time the viability of the cell alone and of the cell in the presence of cisplatin alone

there was no changed based on the dosage (figure 14). There was however a significant difference when it came to the cell viability in the presence of nanoparticles and in the presence of nanoparticles and cisplatin. The cell which received an overall larger amount of cisplatin overtime have a lower cell viability in the presence of nanoparticles. This indicates that the uptake of the nanoparticles was not as successful as it was for the lower overall amount of cisplatin. This reaffirms the earlier discussed idea that as the amount of prior cisplatin exposure increases the uptake of the nanoparticle decreases. The cell with the overall larger amount of cisplatin over time however has a higher cell viability in the presence of nanoparticles and cisplatin. This indicates that the larger the overall exposure to cisplatin the higher the resistivity. A greater uptake of nanoparticles however could lead to a lower cell viability.

Zeta Potential Analysis

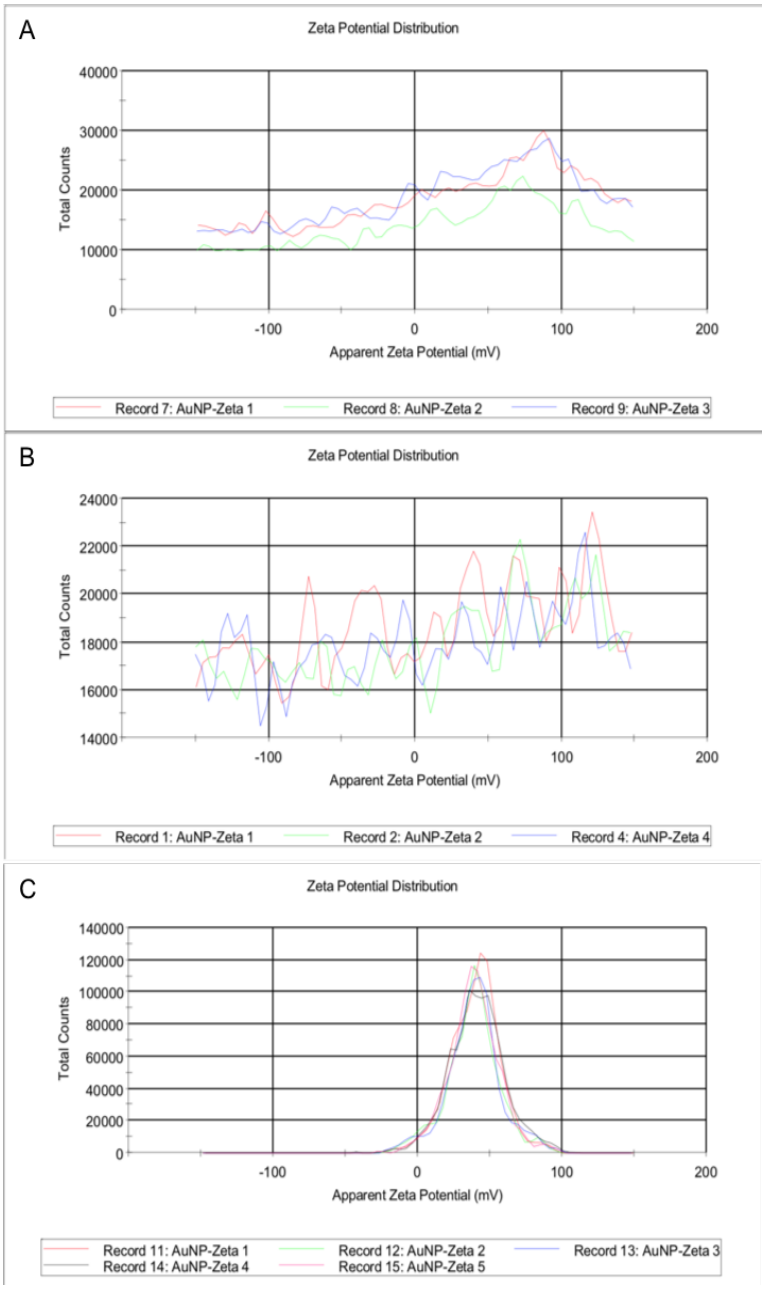

Figure 14. *A: The zeta potential for the 100% PEG conjugated nanoparticle was calculated. The average was found to be 2.03 mV. B: The zeta potential for the 50% PEG/50% RGD conjugated nanoparticle was calculated. The average was found to be 7.75 mV. C: The zeta potential for the 50% PEG /30% RGD/ 20% NLS conjugated nanoparticle was calculated. The average was found to be 40.3 mV.*

The zeta potential was determined for each different conjugation of the conjugations of nanoparticles. In the case of the 2,000 g/mol PEG conjugations both the 100% PEG and the 50% PEG 50% RGD there appears to be a higher standard deviation in the zeta potential as it ranges more wildly from -100 to 100 mV. The 50% PEG/ 30% RDG/ 20% NLS however produced the nice expected gaussian curve with an average zeta potential of 40.3 mV (figure 15). While the PEG and PEG/RGD conjugations are both well within the potential range for neutral nanoparticles, the PEG/RGD/NLS conjugation is just outside of the range of neutrality indicating that it has cation charge on its surface. In this case it appears as though the introduction of RGD slightly increased the zeta

potential while the introduction of NLS vastly increased the zeta potential. The zeta potential graphs for the 5,000 g/mol PEG conjugations all more closely resembled a gaussian curve than that of the 2,000 g/mol PEG conjugations. Similarly, however the curve of the PEG/RGD/NLS is the most gaussian while both the PEG and PEG/RGD experienced some slight shifts. The 100% PEG was found to have an average zeta potential of 35.4 mV (figure 16). This is statistically significantly higher than that of the 2,000 g/mol conjugated 100% PEG according to an ANOVA test giving a p value of .00087. The zeta potential for the 50% PEG/ 50% RGD was found to be 30.9 mV (figure 2). This is also significantly higher than that of the 2,000 g/mol PEG. This is however a decrease from the 100% PEG indicating that the presence of RGD decreases the overall zeta potential. The zeta potential of the 50% PEG/30% RGD/ 20% NLS was found to be 37.3 mV (figure 16). This is a slight increase from that of the other 5,000 g/mol PEG conjugations.

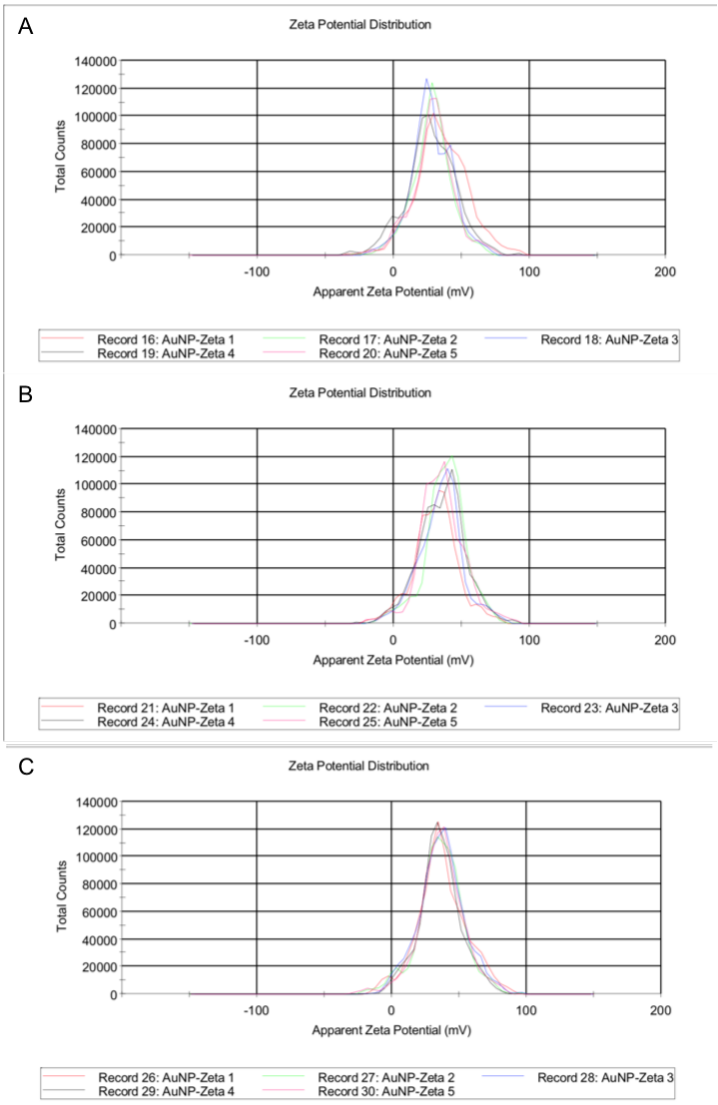

Figure 15. *A: The zeta potential for the 100% PEG conjugated nanoparticle was calculated. The average was found to be 35.4 mV. B: The zeta potential for the 50% PEG/50% RGD conjugated nanoparticle was calculated. The average was found to be 30.9 mV. C: The zeta potential for the 50% PEG /30% RGD/ 20% NLS conjugated nanoparticle was calculated. The average was found to be 37.3 mV.*

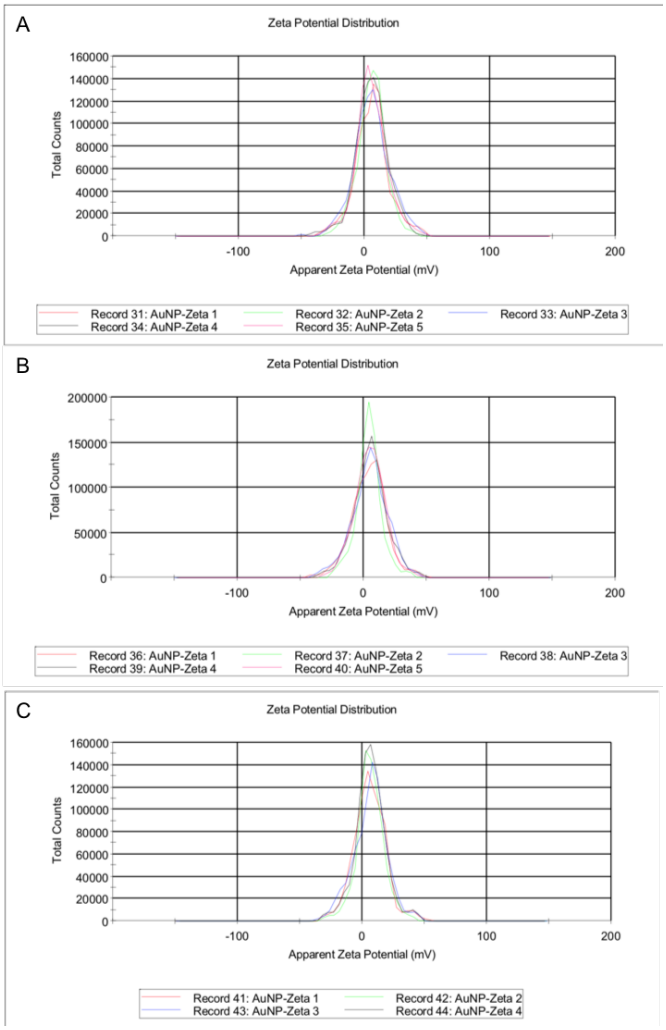

Figure 16. *A: The zeta potential for the 100% PEG conjugated nanoparticle was calculated. The average was found to be 6.13 mV. B: The zeta potential for the 50% PEG/50% RGD conjugated nanoparticle was calculated. The average was found to be 4.32 mV. C: The zeta potential for the 50% PEG /30% RGD/ 20% NLS conjugated nanoparticle was calculated. The average was found to be 6.25 mV.*

This however is a slight decrease from the similarly conjugated 2,000 g/mol which had a zeta potential of 40.3 mV for the 50% PEG/30% RGD/ 20% NLS conjugation. When looking at zeta potentials for the 10,000 g/mol conjugations similar trends were seen. All three of these zeta potential measurements displayed the expected gaussian curves. The zeta potential for the 100% PEG was 6.13 mV (figure 17). The zeta potential for the 50% PEG 50% RGD was found to be 4.32 mV. This shows the same decrease that was present in the 5,000 g/mol conjugation when RDG was added as a ligand. In the case of the 50% PEG/30% RGD/ 20% NLS conjugation the zeta potential was found to be 6.25 mV. This is again the same trend as was seen in the 5,000 g/mol conjugations. All these zeta potentials fall into the neutral range for nanoparticles and in turn have no significant charge associated with the surface.

Dynamic Light Scattering for Analysis of the Radius of the Nanoparticles

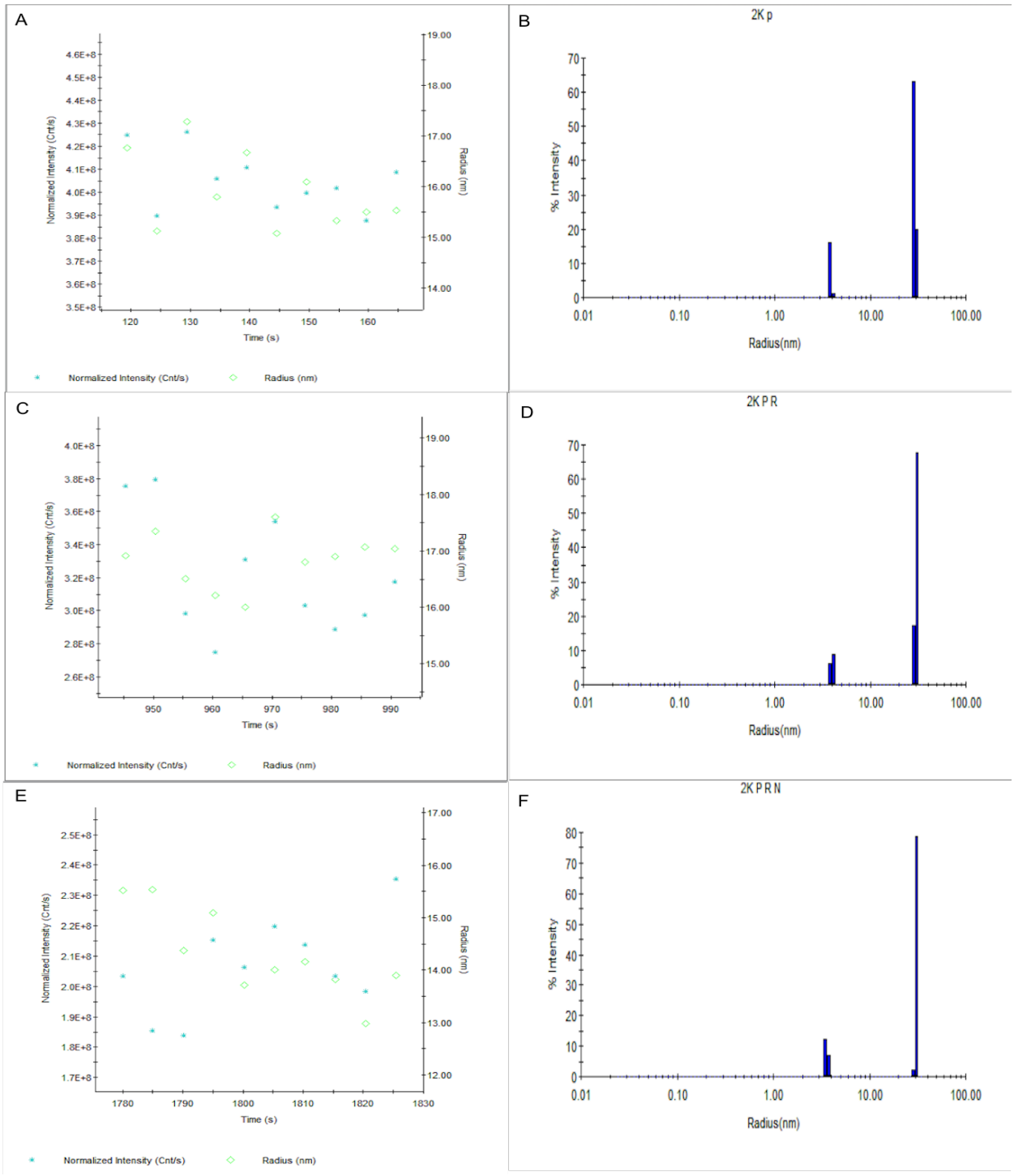

Figure 17. *The radius of the individual nanoparticles was measured using dynamic light scattering. A: The radius was measure 10 separate times for the 100% PEG conjugated nanoparticles. The normalized intensity was also measured. B: The relative intensities of each measured radius for the 100% PEG. C: The radius was measure 10 separate times for the 50% PEG/50% RGD conjugated nanoparticles. The normalized intensity was also measured. D: The relative intensities of each measured radius for the 50% PEG/50% RGD. E: The radius was measure 10 separate times for the 50% PEG/30% RGD/20%NLS conjugated*

nanoparticles. The normalized intensity was also measured. F: The relative intensities of each measured radius for the 50% PEG/30% RGD/20%NLS.

For each of the different conjugations the average radius was plotted along with the relative intensities for each radius (figure 18). In each of the different conjugations there is a small intensity at a smaller radius along with a much larger intensity at a larger radius. The smaller radius could indicate nanoparticles that were not fully covered by ligands. In the case of the 100% PEG conjugated nanoparticles the radius was found to be 25.02 nm. When the conjugation was changed to 50% PEG/ 50% RGD the average radius increased to 26.87 nm and when changed to 50% PEG/30% RGD/20%NLS the average radius was 26.138 nm. The addition of RGD causes a slight increase in the average radius. The average radius in the presence of both RGD and NLS was slightly larger than that of only PEG but still not as large as the 50% PEG/ 50% RGD conjugation. This indicates that it is the RGD that is the cause of the increase in radius. When the amount of RGD conjugated decreases, as it does when the percent of RGD drops from 50% to 30%, it leads to a slight decrease in the radius as analyzed by a t test with a p value of .0091.

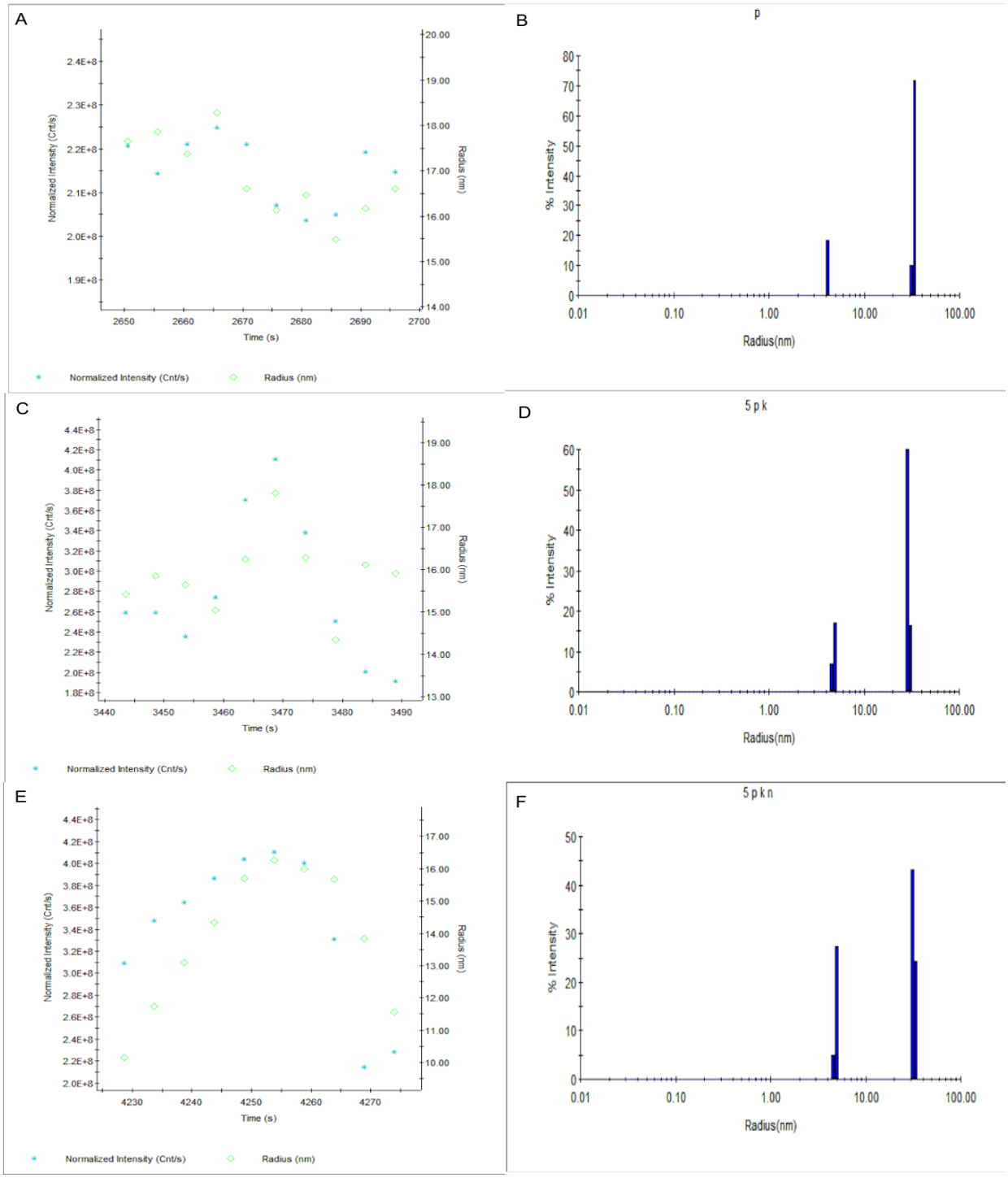

Figure 18 . *The radius of the individual nanoparticles was measured by dynamic light scattering. A: The radius was measure 10 separate times for the 100% PEG conjugated nanoparticles. The normalized intensity was also measured. B: The relative intensities of each measured radius for the 100% PEG. C: The radius was measure 10 separate times for the 50% PEG/50% RGD conjugated nanoparticles. The normalized intensity was also measured. D: The relative intensities of each measured radius for the 50% PEG/50% RGD. E: The radius was measure 10 separate times for the 50% PEG/30% RGD/20%NLS conjugated nanoparticles. The normalized intensity was also measured. F: The relative intensities of each measured radius for the 50% PEG/30% RGD/20%NLS.*

In the 5,000 g/mol a similar pattern was seen in the distribution of the of radii. Again, there is a less intense measurement with a smaller radius along with a more intense measurement at a higher radius. When looking at the 5,000 g/mol conjugations the 100% PEG conjugation had an average radius of 28.74 nm. This is significantly larger than that of the 2,000 g/mol conjugation indicating that the increase in chain length leads to an increase in overall size. When changing the conjugation to 50%PEG/ 50% RGD the radius dropped to 23.54 nm while the 50% PEG/30% RGD/20%NLS conjugation had an average radius of 23.69 nm. This indicates that the presence of RGD decreases the radius. When there is less of a percentage of RGD as there is in the 50% PEG/30% RGD/20%NLS conjugation the radius did not experience quite as much decrease.

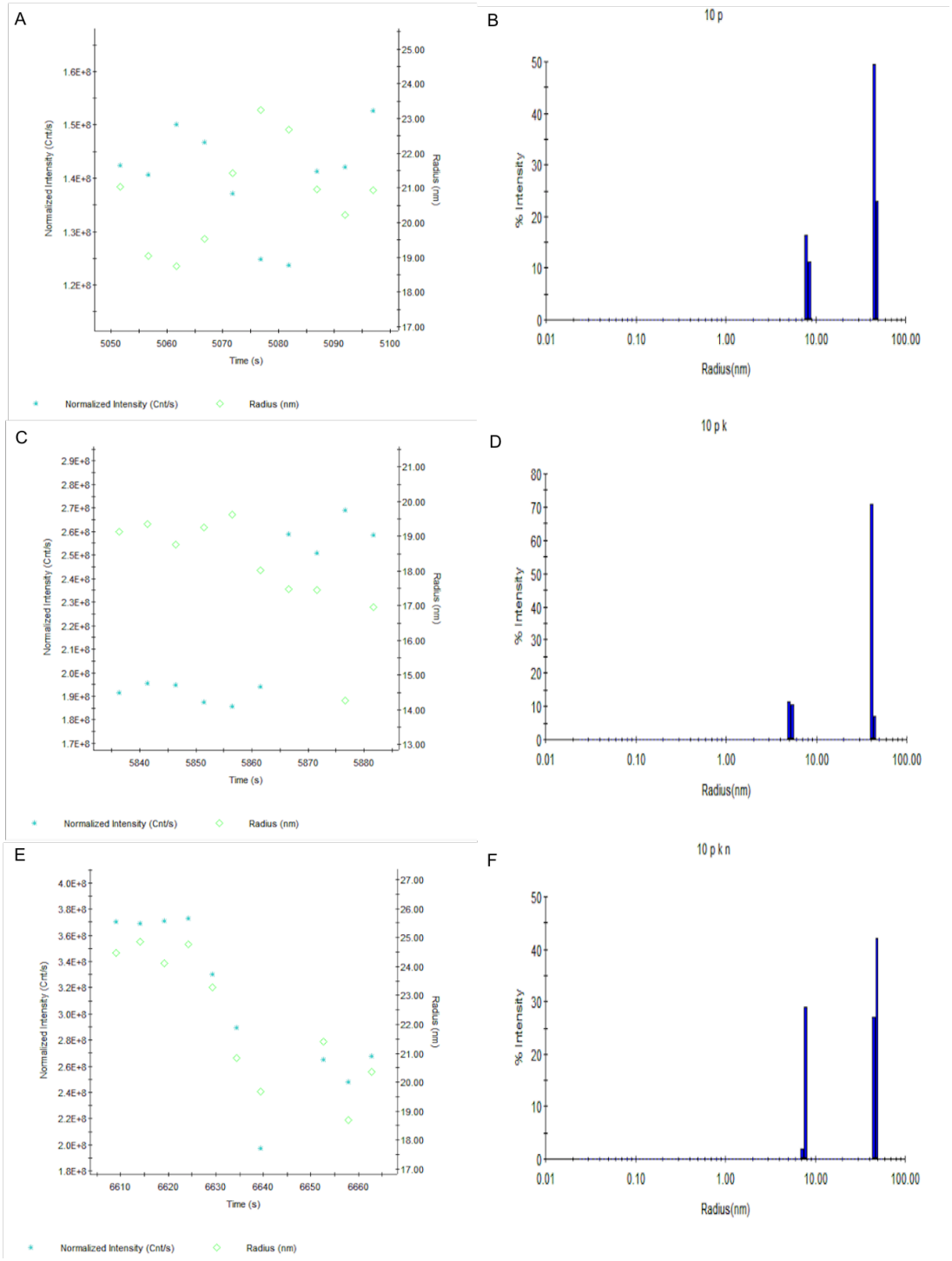

Figure 19. *The radius of the individual nanoparticles was measured by dynamic light scattering. A: The radius was measure 10 separate times for the 100% PEG conjugated nanoparticles. The normalized intensity was also measured. B: The relative intensities of each measured radius for the 100% PEG. C: The radius was measure 10 separate times for the 50% PEG/50% RGD conjugated nanoparticles. The normalized intensity was also measured. D: The relative intensities of each measured radius for the 50% PEG/50% RGD. E: The radius was measure 10 separate times for the 50% PEG/30% RGD/20%NLS conjugated nanoparticles. The normalized intensity was also measured. F: The relative intensities of each measured radius for the 50% PEG/30% RGD/20%NLS.*

As with the 2,000 and 5,000 g/mol conjugations there are two separate intensities, a smaller one with a lower radius and a more intense one with a higher radius. The 100% PEG conjugation for the 10,000 g/mol had an average radius of 36.16 nm. This is higher than that of the 2,000 g/mol and the 5,000 g/mol. This indicates that increasing the chain length increases the overall radius. The 50% PEG/ 50% RGD conjugation has an average radius of 33.92 nm. This reaffirms the trend observed in the 5,000 g/mol that the presence of RGD decreases the overall average radius. When the conjugation changes to 50%PEG/30%RGD/20%NLS the radius increased back up to 35.67 nm. This again reaffirms the trend observed in the 5,000 g/mol that by decreasing the RGD percentage the radius increased.

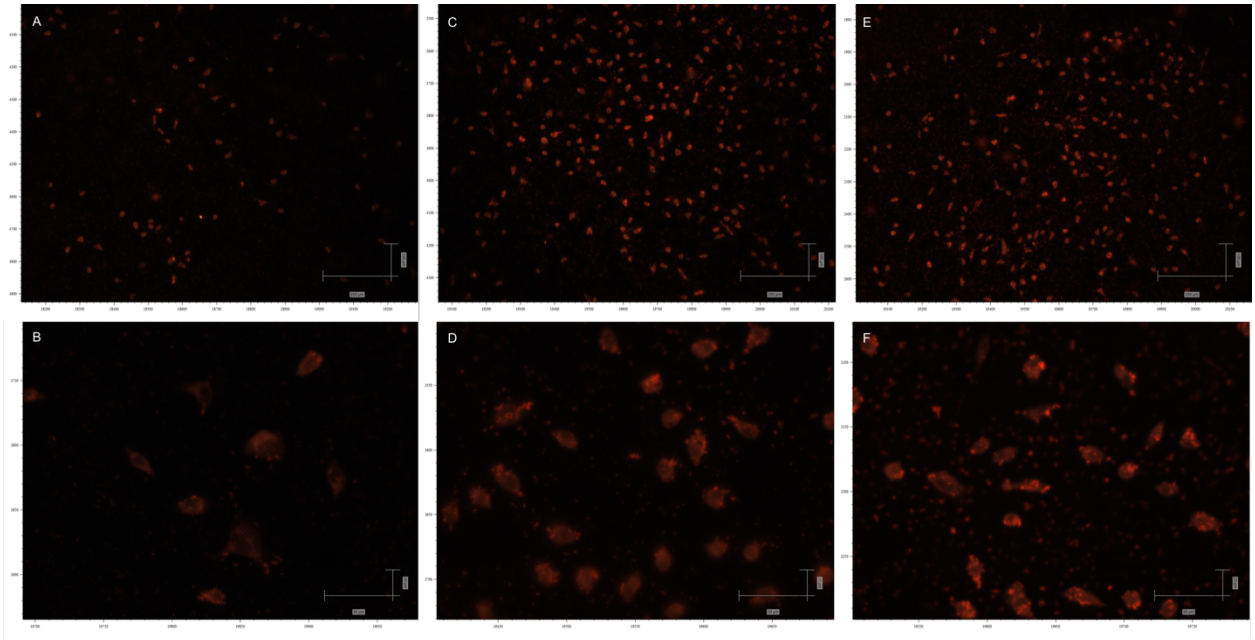

Figure 20. *Uptake of 2,000 g/mol conjugated nanoparticles: A: HSC cells with nanoparticles with 100% PEG at a 5x magnification. B: HSC cells with nanoparticles with 100% PEG at a 20x magnification. C: HSC cells with nanoparticles with 50% PEG/50% RGD at a 5x magnification. D: HSC cells with nanoparticles with 50% PEG/50%RGD at a 20x magnification. E: HSC cells with nanoparticles with 50% PEG/30%RGD/20%NLS at a 5x magnification. F: HSC cells with nanoparticles with 50% PEG/30%RGD/20%NLS at a 20x magnification.*

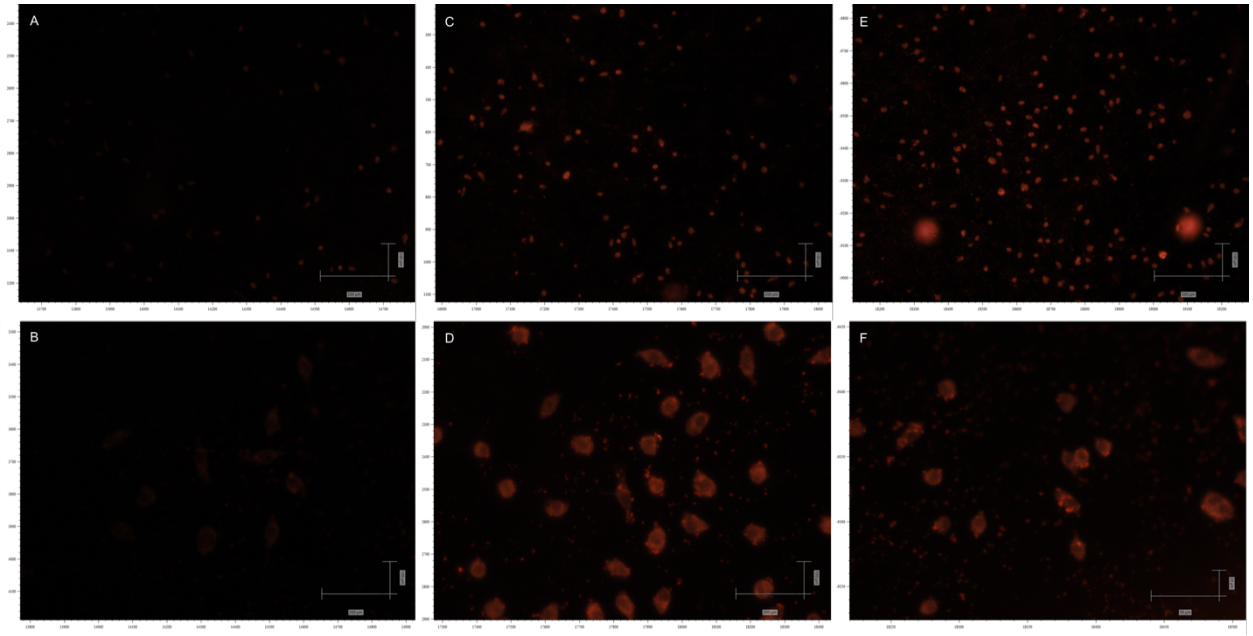

Figure 21. *Uptake of 5,000 g/mol conjugated nanoparticles: A: HSC cells with nanoparticles with 100% PEG at a 5x magnification. B: HSC cells with nanoparticles with 100% PEG at a 20x magnification. C: HSC cells with nanoparticles with 50% PEG/50% RGD at a 5x magnification. D: HSC cells with nanoparticles with 50% PEG/50%RGD at a 20x magnification. E: HSC cells with nanoparticles with 50% PEG/30%RGD/20%NLS at a 5x magnification. F: HSC cells with nanoparticles with 50% PEG/30%RGD/20%NLS at a 20x magnification.*

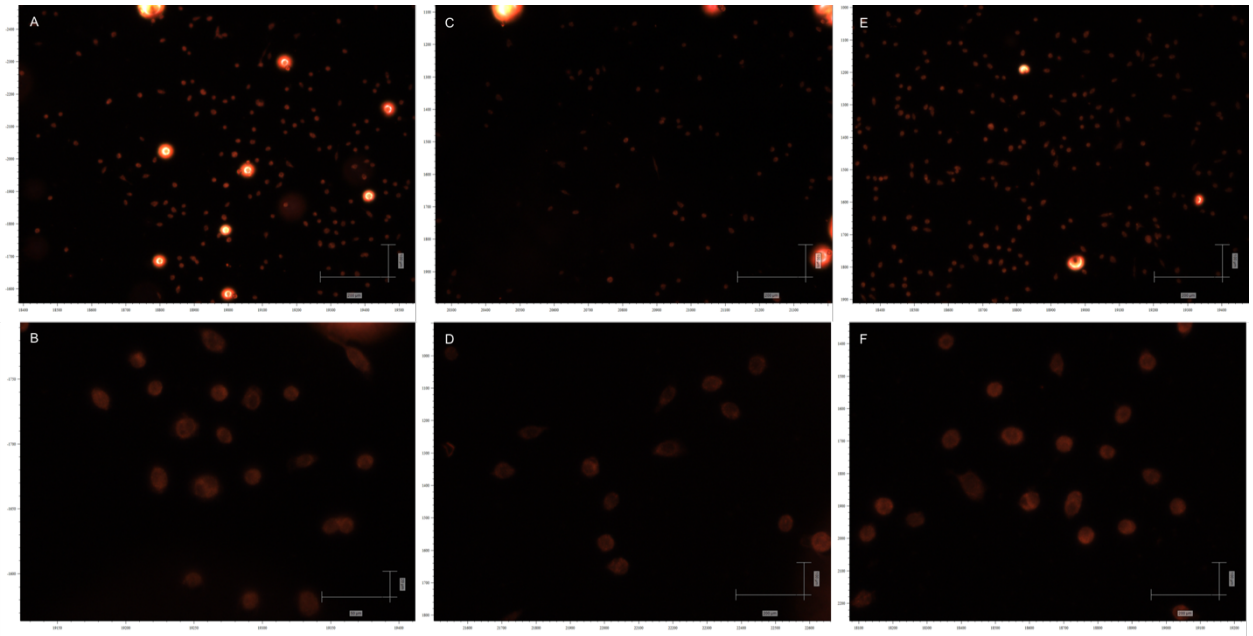

Figure 22. *Uptake of 10,000 g/mol conjugated nanoparticles: A: HSC cells with nanoparticles with 100% PEG at a 5x magnification. B: HSC cells with nanoparticles with 100% PEG at a 20x magnification. C: HSC cells with nanoparticles with 50% PEG/50% RGD at a 5x magnification. D: HSC cells with nanoparticles with 50% PEG/50%RGD at a 20x magnification. E: HSC cells with nanoparticles with 50% PEG/30%RGD/20%NLS at a 5x magnification. F: HSC cells with nanoparticles with 50% PEG/30%RGD/20%NLS at a 20x magnification.*

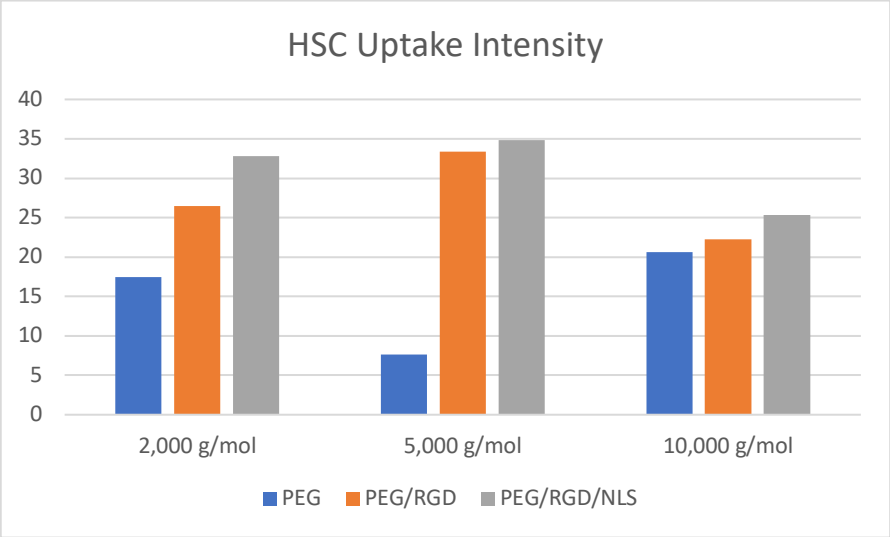

Figure 23. *Intensity of Uptake: The intensity of the uptake of the differently conjugated nanoparticles was measured and analyzed. Each different conjugation was compared within itself and across different lengths.*

The relative intensities of each of the different conjugated nanoparticles was analyzed. As expected, the PEG only conjugation had the lowest uptake intensity regardless of the length of the PEG followed by the uptake of nanoparticles with PEG and RGD with the nanoparticles with all PEG RGD and NLS having the highest uptake of them all. Without the presence of RGD or NLS 10,000 g/mol had the highest uptake while 5,000 g/mol had the lowest. However, with the addition of RGD and NLS the 10,000 g/mol had the lowest uptake with the 5,000 g/mol had the highest uptake as concluded by an ANOVA test with a p value of .041.

Changes in Cisplatin Resistant Cells

The uptake of the conjugated nanoparticles may be decreased in cisplatin resistant human oral squamous cell carcinoma cells, HSC-3, as compared to non-resistant HSC-3 cells. This implication would lead to photothermal therapy, a therapy that is used to kill localized cancer tumors through heating of the nanoparticles to be less effective as less nanoparticles would be present in the cells. The decrease in nanoparticle uptake was not the only change that was seen with the cisplatin resistant cells. A noticeable morphological change was seen along with changes in growth time as the HSC-3 cells were exposed to cisplatin. This semester cisplatin resistant cells were cultured the

same as previously done with the cells being exposed to small amounts of cisplatin with each new culture. Unlike last time however, the growth time was recorded to determine how the exposure to cisplatin effects the growth rate. The growth rates were combined into the table and graph below.

Table 3. *Growth Rate Following Exposure to Cisplatin The number of days to 85% confluence was analyzed with each subsequent culturing of the HSC-3 cells.*

EXPOSURES TO CISPLATIN	AVERAGE DAYS TO 85% CONFLUENCE
0	3.7
1	4.1
2	8.7
3	22.5

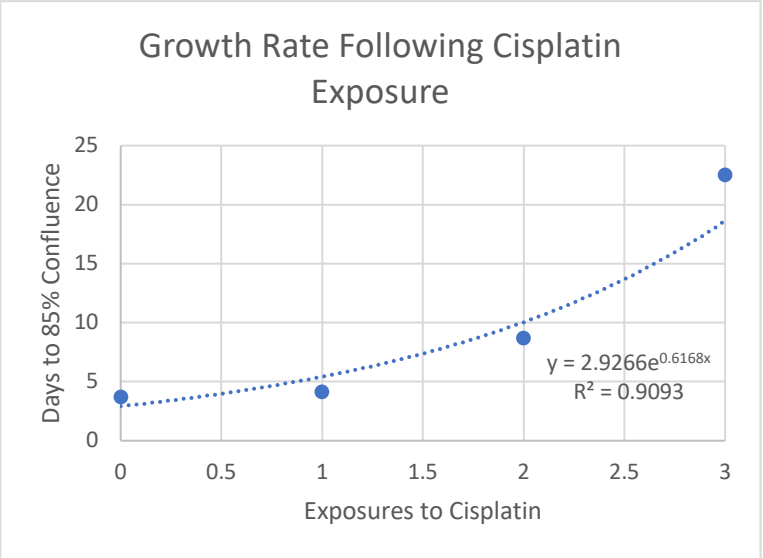

Figure 24. *Growth Rate Following Exposure to Cisplatin (right): The growth rates were plotted against the number of exposures to cisplatin. It was determined that cisplatin has an exponential effect on growth rate.*

The exposure to cisplatin is seen to have an exponential effect on the growth rate of the HSC-3 cells. As cisplatin works as a chemotherapeutic by causing DNA damage the path to which resistance occurs is still relatively unknown, however from these experiments it was found that cisplatin resistant cells experience changes to their growth cycle even from one exposure. In addition, the uptake of nanoparticles was studied in nonresistant and cisplatin resistant HSC-3 cells to find out if in fact uptake was decreased for resistant cells.

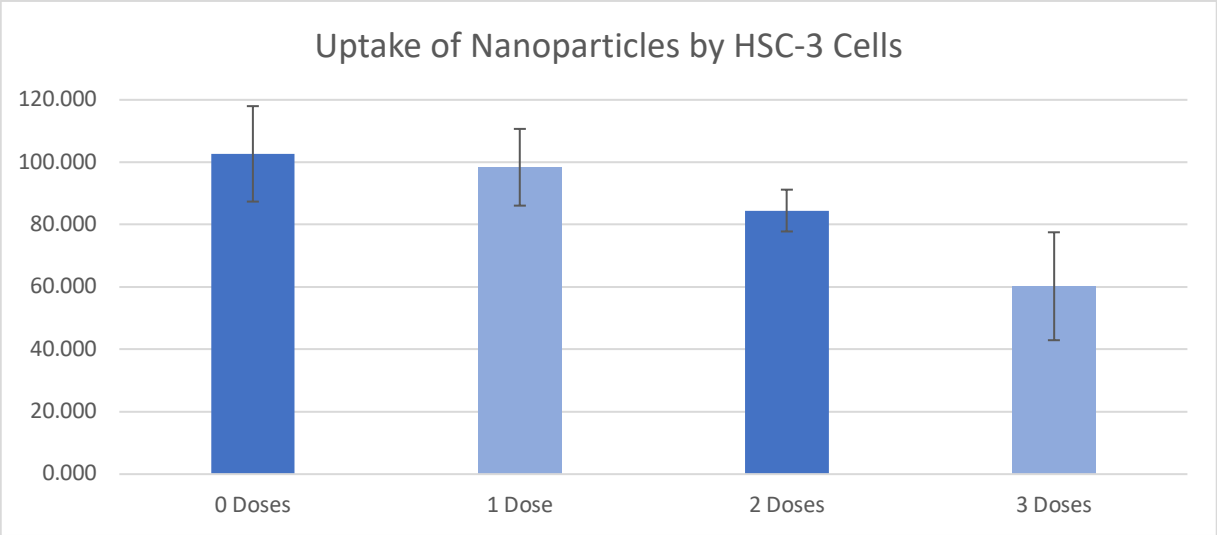

Figure 25. *Cells were cultured and exposed to cisplatin for a various number of times. The cells were exposed to the same amount of nanoparticles before analysis via dark field imaging and ImageJ.*

The pattern that was seen in the changes in growth rate based on exposure to cisplatin is seen again through the uptake of nanoparticles. Though there is some changed from the first exposure to cisplatin, by the time the HSC-3 cells have been dosed three times the decrease in uptake is more drastic. As the patterns are the same for both the growth rate and the uptake of the nanoparticles this indicates that the two may be correlated. One explanation is that when cisplatin interacts with the cell and causes the resistance the surface of the HSC-3 cells is being altered. This alteration could be either on an intramembranous pump or on the charge of the surface itself. These changes would lead to different interactions between the nanoparticles leading to difference in uptake while simultaneously changing how long it takes for the cell to grow. More data would need to be able to draw any definitive conclusions.

Conclusions and Future Work

The uptake of nanomaterial into cells can be promoted using different ligands on the nanoparticles. By binding ligands to the nanoparticle, it not only protected the nanoparticle but also the cell. For spheres the best uptake was experienced when the nanospheres were bound with PEG, RGD and NLS. For cubes the best uptake was experienced when the nanocubes were bound with only PEG and RGD. Overall the HSC-3 cells experienced more uptake than the MDA-MB-231 cells indicating that this combination of ligands was better suited for the HSC-3 cells as validated by statistical analysis. A different ratio of the current ligands or a different combination of ligands all together might lead to better uptake in the MDA-MB-231 cells. Since these are different cell lines it is expected for them to experience different uptakes as shown by the different intensities observed. Through additional experimentation a more precise reason for this phenomenon could be explained.

The effects of the addition of nanoparticles on the mobility of HSC cells can be analyzed in respect to both its position and its velocity. The introduction of chemotherapeutic drugs often causes the cells to increase their velocity and scatter before the drug kills the cell as validated by statistical analysis. This is dangerous as the movement of cancer cells rapidly allows them to move to other parts of the body, thus continuing the spread of cancer. The presence of nanoparticles alone restricts the displacement of the HSC cells. Nanoparticles are an effective means of restricting the movement of the HSC cells and slowing the progress. The implications of this allow the targeting of cells which in turn would allow the treatment of cancer cells with reduced spreading before apoptosis. The introduction of cisplatin to the HSC cells causes an increase in mobility. With a higher concentration causing greater movement the cells are still experiencing movement great

enough to allow the cells to move from a central site to a previously non-cancerous site. The optimization of the concentration of the cisplatin should be obtained to determine the concentration of which an increase would cause more harm than good. Further experimentation would need to be run to understand the underlying effects with produce this result. While the introduction of cisplatin into the cells causes an increase in the mobility of the cells, coupled with the use of nanoparticles it may be used to effectively treat cancer without increasing the spread. The optimal concentration of cisplatin should be obtained from further experimentation to determine the correct ratios to use.

The different chain lengths of the PEG along with the presence of RGD and NLS lead to differences in the zeta potential, radius size, and uptake intensity. With the addition of RGD all the different chain lengths experienced a decrease in zeta potential and the addition of NLS caused the zeta potential to increase. It was seen that overall the 5,000 g/mol had the highest zeta potential while both the 2,000 and 10,000 both remained in the neutral range for surface charge. The 5,000 g/mol however had the highest nanoparticle uptake indicating that some surface charge might be beneficial to increase uptake as validated by statistical analysis. Not all the chain lengths experienced the same trends regarding the average radius. The 2,000 g/mol experienced an increase in average radius with the addition of RGD while both the 5,000 g/mol and the 10,000 g/mol experienced a decrease. Both however experienced a larger radius that the 2,000 g/mol initially as expected. This indicates that the RGD may have a longer length than the 2,000 g/mol but shorter than the 5,000 g/mol and 10,000 g/mol. As expected, the PEG/RGD/NLS conjugations had the highest uptake with the PEG conjugations being the lowest. The 5,000 g/mol showed the

highest uptake overall indicating that there is a tradeoff between the size of the nanoparticle and the charge associated with it.

Repeated and constant exposure to cisplatin has many effects on HCS cells. Not only does the exposure lead to a resistance but it also leads to growth and structural differences as indicated by preliminary data. This is indicative of the multiple ways in which cisplatin interacts with HSC cells and as such leads to a difficult resistivity to assess. As the number of prior doses of cisplatin increases in the presence of cisplatin alone the resistivity remains the same for all resistant cells. The difference in the cell viability across different cells comes into play once the nanoparticles are introduced. The use of nanoparticles often increases the amount of cisplatin and in turn leads to a lower cell viability as more cells are killed due to the cisplatin. The structural changes that accompany the HSC cells as their exposure to cisplatin increases leads to a reduction in the amount of nanoparticles that can be uptaken by the cells. The presence of nanoparticles preliminarily leads to a higher cell viability despite their uptake overtime slowing. With an altered nanoparticle it may be possible to induce more uptake into the HSC cells with more exposure and in turn lower their cell resistivity combating the resistance which they have built up. While it is not the cisplatin itself but the nanoparticle that the HSC cells are treated with in addition to the cisplatin that makes the difference this indicates that a difference in nanoparticles could be able to combat cisplatin resistance. Though it is clear throughout the study that cisplatin resistance has a clear effect on the uptake of the nanoparticles by the cells a more thorough understanding and analysis of the resistance would allow for further insights on how to overcome this barrier. Once the nanoparticles can overcome the resistance this would allow for an expansion of photothermal treatment to cancers that have previously been treated with cisplatin.

References

1. Wang, E. C.; Wang, A. Z., NANOPARTICLES AND THEIR APPLICATIONS IN CELL AND MOLECULAR BIOLOGY. *Integr Biol (Camb)* **2014,** *6* (1), 9-26.
2. Cho, K.; Wang, X.; Nie, S.; Chen, Z.; Shin, D. M., Therapeutic Nanoparticles for Drug Delivery in Cancer. *Clinical Cancer Research* **2008,** *14* (5), 1310-1316.
3. Taylor, U.; Tiedemann, D.; Rehbock, C.; Kues, W. A.; Barcikowski, S.; Rath, D., Influence of gold, silver and gold–silver alloy nanoparticles on germ cell function and embryo development. *Beilstein Journal of Nanotechnology* **2015,** *6*, 651-64.
4. Dasari, S.; Tchounwou, P. B., Cisplatin in cancer therapy: molecular mechanisms of action. *European journal of pharmacology* **2014,** *740*, 364-78.
5. Duan, X.; He, C.; Kron, S. J.; Lin, W., Nanoparticle formulations of cisplatin for cancer therapy. *Wiley interdisciplinary reviews. Nanomedicine and nanobiotechnology* **2016,** *8* (5), 776-91.
6. Sastry, J.; Kellie, S. J., SEVERE NEUROTOXICITY, OTOTOXICITY AND NEPHROTOXICITY FOLLOWING HIGH-DOSE CISPLATIN AND AMIFOSTINE. *Pediatric Hematology and Oncology* **2005,** *22* (5), 441-445.
7. Engel, J.; Schonenberger, H.; Lux, F.; Hilgard, P., Estrophilic cisplatin derivatives. *Cancer Treatment Reviews* **1987,** *14* (3), 275-283.
8. Shen, D. W.; Pouliot, L. M.; Hall, M. D.; Gottesman, M. M., Cisplatin resistance: a cellular self-defense mechanism resulting from multiple epigenetic and genetic changes. *Pharmacological reviews* **2012,** *64* (3), 706-21.
9. Duan, G.; Tang, Q.; Yan, H.; Xie, L.; Wang, Y.; Zheng, X. E.; Zhuge, Y.; Shen, S.; Zhang, B.; Zhang, X.; Wang, J.; Wang, W.; Zou, X., A Strategy to Delay the Development of Cisplatin Resistance by Maintaining a Certain Amount of Cisplatin-Sensitive Cells. *Scientific reports* **2017,** *7* (1), 432.
10. Ciarimboli, G., Membrane transporters as mediators of Cisplatin effects and side effects. *Scientifica* **2012,** *2012*, 473829.
11. Akash, M. S. H.; Rehman, K.; Chen, S., Polymeric-based particulate systems for delivery of therapeutic proteins. *Pharmaceutical Development and Technology* **2016,** *21* (3), 367-378.
12. Dykman, L.; Khlebtsov, N., Gold Nanoparticles in Biology and Medicine: Recent Advances and Prospects. *Acta Naturae* **2011,** *3* (2), 34-55.
13. Dickerson, E. B.; Dreaden, E. C.; Huang, X.; El-Sayed, I. H.; Chu, H.; Pushpanketh, S.; McDonald, J. F.; El-Sayed, M. A., Gold nanorod assisted near-infrared plasmonic photothermal therapy (PPTT) of squamous cell carcinoma in mice. *Cancer Lett* **2008,** *269* (1), 57-66.
14. Miller, M. A., Gold photothermal therapy: A positive for negative margins. *Science Translational Medicine* **2018,** *10* (423), eaar7512.
15. Qian, W.; Curry, T.; Che, Y.; Kopelman, R. In *Targeted delivery of peptide-conjugated biocompatible gold nanoparticles into cancer cell nucleus*, SPIE BiOS, SPIE: 2013; p 8.
16. Kallay, N.; Žalac, S., Stability of Nanodispersions: A Model for Kinetics of Aggregation of Nanoparticles. *Journal of Colloid and Interface Science* **2002,** *253* (1), 70-76.
17. Shenoy, D.; Fu, W.; Li, J.; Crasto, C.; Jones, G.; DiMarzio, C., Surface functionalization of gold nanoparticles using hetero-bifunctional poly(ethylene glycol) spacer for intracellular tracking and delivery. **2006,** *1* (1), 51-7.

18. Hauck, T. S.; Ghazani, A. A.; Chan, W. C. W., Assessing the Effect of Surface Chemistry on Gold Nanorod Uptake, Toxicity, and Gene Expression in Mammalian Cells. *Small* **2008,** *4* (1), 153-159.
19. Clogston, J. D.; Patri, A. K., Zeta Potential Measurement. In *Characterization of Nanoparticles Intended for Drug Delivery*, McNeil, S. E., Ed. Humana Press: Totowa, NJ, 2011; pp 63-70.
20. Wang, E. C.; Wang, A. Z., Nanoparticles and their applications in cell and molecular biology. *Integr Biol (Camb)* **2014,** *6* (1), 9-26.
21. Guo, S.; Wang, Y.; Miao, L.; Xu, Z.; Lin, C. M.; Zhang, Y.; Huang, L., Lipid-Coated Cisplatin Nanoparticles Induce Neighboring Effect and Exhibit Enhanced Anticancer Efficacy. *ACS Nano* **2013,** *7* (11), 9896-904.
22. Bellis, S. L., Advantages of RGD peptides for directing cell association with biomaterials. *Biomaterials* **2011,** *32* (18), 4205-10.
23. Panikkanvalappil, S. R.; Hooshmand, N.; El-Sayed, M. A., Intracellular Assembly of Nuclear-Targeted Gold Nanosphere Enables Selective Plasmonic Photothermal Therapy of Cancer by Shifting Their Absorption Wavelength toward Near-Infrared Region. *Bioconjugate Chemistry* **2017,** *28* (9), 2452-2460.
24. Dasari, S.; Tchounwou, P. B., Cisplatin in cancer therapy: molecular mechanisms of action. *European journal of pharmacology* **2014,** *0*, 364-78.
25. Nikoobakht, B.; El-Sayed, M. A., Preparation and Growth Mechanism of Gold Nanorods (NRs) Using Seed-Mediated Growth Method. *Chemistry of Materials* **2003,** *15* (10), 1957-1962.
26. Wei, Q.; Xiaohua, H.; Bin, K.; Mostafa, A. E.-S., Dark-field light scattering imaging of living cancer cell component from birth through division using bioconjugated gold nanoprobes. *Journal of Biomedical Optics* **2010,** *15* (4), 1-9.
27. Thawing, Propagating, and Cryopresserving Protocol. 1.5 ed.; Collection, A. T. C., Ed. 2012.
28. Wang, W.; Ding, X.; Xu, Q.; Wang, J.; Wang, L.; Lou, X., Zeta-potential data reliability of gold nanoparticle biomolecular conjugates and its application in sensitive quantification of surface absorbed protein. *Colloids and Surfaces B: Biointerfaces* **2016,** *148*, 541-548.
29. Zheng, T.; Bott, S.; Huo, Q., Techniques for Accurate Sizing of Gold Nanoparticles Using Dynamic Light Scattering with Particular Application to Chemical and Biological Sensing Based on Aggregate Formation. *ACS Applied Materials & Interfaces* **2016,** *8* (33), 21585-21594.